Biocarbon materials

Amar K. Mohanty[1,2] ✉ Singaravelu Vivekanandhan[3], Oisik Das[4], Lina M. Romero Millán[5], Naomi B. Klinghoffer[6,7], Ange Nzihou[8,9] & Manjusri Misra[1,2]

Abstract

Biocarbons are carbonaceous solids derived from renewable and sustainable feedstocks and their combinations through thermochemical conversion at high temperatures (>350 °C) in the absence of oxygen or in limited oxygen. Expanding their applications from soil and fuel into advanced arenas of polymer composites, energy and environment is the key strategy to substitute for a wide range of conventional fossil-based carbon materials with the added benefits of sustainability and circularity. This Primer discusses biocarbon research, including feedstock selection, characterization, pyrolysis techniques, post-modification strategies, diversified applications and challenges. A critical assessment of carbon sequestration, waste reduction, economic impact, material sustainability and circularity and future perspectives is presented. This Primer mainly focuses on materials (polymer composites), energy (storage and conversion) and environmental remediation (wastewater treatment and CO_2 capture). The hurdles that biocarbon-based materials must overcome are effective market propagation, industry-standard adherence and maintenance of a steady flow of feedstocks to guarantee continuous production. Maintenance of reproducibility of biocarbon materials with similar physicochemical and functional properties is another challenging task, which needs more investigation with the support of theoretical modelling and database generation. The Primer also delves into techno-economic analysis, which integrates biomass logistics and their industrial processing, which will enable a new manufacturing platform in biocarbon production for large-scale technological applications.

Introduction

Pyrolysis is a thermochemical conversion of ligno-cellulosic biomass and other waste materials (at 350 °C and above) in the absence of oxygen or in limited oxygen. The solid fractions of the pyrolytic process, biocarbon or biochar, are gaining increasing importance owing to their renewable nature, structural and morphological diversity, and physicochemical properties with similarity to conventional fossil resource-based carbon materials[1]. Increasing demand for sustainable materials with superior properties and climate change benefits triggered the exploration of biocarbon for a diverse range of applications including materials, energy and environmental remediation, beyond their conventional uses as fuel and soil conditioner[1–3]. Biocarbon is produced through various thermochemical processes using different types of renewable and sustainable feedstock, such as biomass and plastic wastes[4,5]. Appropriate selection of renewable and/or sustainable feedstock and the thermochemical conversion process, influences the formation of various biocarbon materials including biochar, engineered biocarbons and biocarbon nanostructures[6,7]. Biocarbon has the potential to alleviate the challenges associated with fossil fuel-derived precursors such as high cost, limited and/or localized reserve and greenhouse gas emissions.

Biocarbon materials are being used in many novel applications, such as reinforcement in polymeric composites[8], active electrode or conducting carbon in energy storage[9,10], physisorption agent in hydrogen storage[11], oxygen reduction reaction (ORR) catalyst in fuel cell technologies[12], sensitizer and counter-electrode in dye-sensitized solar cells[13], substrates to support microbial metabolism in H_2 production through anaerobic digestion[14], adsorption medium in wastewater treatment[15] and CO_2 capture[16]. Increased use of biocarbon towards large-volume applications can contribute to the circular economy by enabling waste (agro, forestry, industrial or municipal) valorization, climate change mitigation and carbon sequestration[17–20]. However, one of the main challenges associated with biocarbon lies in achieving the desired physicochemical properties required for specific applications[11]. This can be addressed through careful selection of suitable precursors, implementation of appropriate pyrolysis processes and the application of desired pre- and post-modification treatments[21]. Realization of the relationship between these factors is crucial to attain the desired characteristics of biocarbon. To improve the commercial viability of biocarbon, it is important to have a clear understanding of the various components of the supply chain, including biomass origin and types and availability; transportation, which deals with the delivery of biomass to pyrolysis facilities and the produced biocarbon to various end users; and the reproducibility of the desired properties of the biocarbons.

This Primer gives a brief overview of methods for the synthesis of biocarbon from diverse renewable and sustainable feedstocks, using various thermochemical processes. It summarizes the mechanisms involved in the transformation of biomass into biocarbon and discusses modification techniques to enhance biocarbon properties, suitable for specific applications. The Primer also discusses the structural, morphological and functional characteristics of biocarbon for various applications, focusing on materials (polymer composites), energy (storage and conversion) and environmental remediation (wastewater treatment and CO_2 capture), as depicted in Fig. 1. With such diversity of applications, the benefits of biocarbon pertaining to sustainability and the circular economy are highlighted. The Primer also discusses challenges associated with biocarbon production and use, in terms of supply chain, reproducibility of material properties and the establishment of a global biocarbon database.

Experimentation

Biomass diversity and availability

The key advantages of using biomass as the feedstock for biocarbon materials are its diversity, abundance, carbon-rich constituents and environmental benefits (such as carbon sequestration, waste valorization and greenhouse gas reduction)[7,22]. Numerous types of biomass, namely industrial co-products, municipal clean wastes, agro-forestry residues, energy crops and aquatic biomass, have been investigated as feedstocks for biocarbon production; further details are provided in the Supplementary information[23–26]. Biomass exhibits a diverse range of structural (cellulose, hemicelluloses, lignin, minerals and other components) and morphological features, yielding biocarbons with various physiochemical properties and functionalities[4]. The increasing demand for biocarbon requires consideration of the availability of biomass for large-volume production[3]. Hence, it is essential to have a clear understanding about biomass diversity, its availability and its desired properties to strengthen the supply chain[27].

An increase in agricultural activity is needed to ensure food security for the increasing global population. Agricultural activity is directly proportional to the amount of residual biomass production, which needs to be disposed of or used in an economically effective manner. Forestry-related activities (logging and lumbering), paper and pulp and agro industries also generate a large volume of biomass, and urban day-to-day activities generate organic waste, which needs to be disposed of in an effective manner[28]. Furthermore, aquatic biomass and its residues (from algae biofuel industries and fish processing industries) also contribute to biomass, which can be used for biocarbon production[24]. In recent years, biomass has been combined with a wide range of waste plastics and co-pyrolysed into biocarbon. This approach can be adopted as an effective method of disposal of non-recyclable plastic wastes to avoid landfill and incineration[5]. Apart from the carbon content, moisture and mineral proportion of biomass also influence its quality in terms of oxygen to carbon and hydrogen to carbon ratios along with residual ash. Biomass rich in lignin can produce biocarbon with high carbon content and dominant graphitic features[7,29]. Volatile content is another key biomass parameter, whereby high volatile content may result in low biocarbon yields.

Thermochemical conversion techniques

Biocarbon is produced by thermochemical processing (pyrolysis or carbonization) of biomass-based feedstocks, whereby the feedstock is heated to temperatures greater than 350 °C in the absence of oxygen (or in limited oxygen). Thermochemical conversion lowers the oxygen and hydrogen content of biomass and consequently increases its elemental carbon, energy density and porosity. The feedstock and processing techniques determine the composition of biocarbon; for example, carbon content in biocarbon can range from 44% to 95%, oxygen content can range from 0% to 45% and hydrogen content from 1% to 9%[30]. Processing conditions change the chemical structures, fixed carbon, volatile matter and ash content. In general, longer residence times and higher temperatures increase carbon and ash content, owing to the removal of oxygen and hydrogen. These conditions also increase fixed carbon while decreasing volatile matter.

Pyrolysis. Pyrolysis is classified as slow (<30 °C min^{-1}), fast (30–1,000 °C min^{-1}) or flash (>1,000 °C min^{-1})[4]. A higher heating rate typically results in more liquid products and lower biocarbon production. For example, slow pyrolysis provides bio-oil yields of 20–40%, whereas flash pyrolysis provides bio-oil yields of 75–80%[4]. In terms of biocarbon

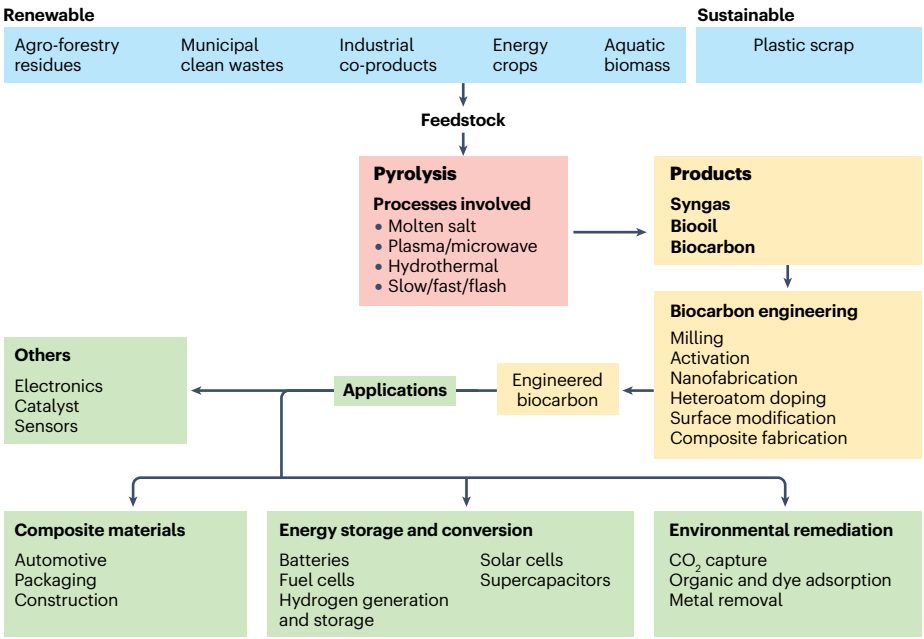

Fig. 1 | Biocarbon materials for composite, energy, environmental and other technological applications. Biomass feedstock can be classified into the following major groups based on origin: agro-forestry residues (biomass generated via various agricultural and forestry activities), industrial co-products (generated from various industrial operations), municipal clean wastes (food waste from restaurants, retail stores and home kitchens) and aquatic biomass. Plastic scrap can serve as a carbon source if mixed with biomass, referred to as sustainable feedstock. Processing techniques consider feedstock diversity, lowering energy demand and tailoring biocarbon properties. Products of biomass pyrolysis include syngas, bio-oil and biocarbon. The yield and quality of these products depend on factors that include biomass nature and pyrolysis conditions such as heating rate, pyrolysis temperature, residence time and sweep gas flow rate. Biocarbon engineering uses various modification techniques to enhance performance. Engineered biocarbons exhibit superior physiochemical, structural, morphological and functional properties compared with their unmodified counterparts.

yield, slow pyrolysis produces ~30% (~400 °C) whereas fast pyrolysis produces 12–26% (~500–1,000 °C) biocarbon[31]. Hence, flash pyrolysis is generally not used for biocarbon production. High-temperature pyrolysis, which takes place at temperatures above 900 °C, produces biocarbon with a higher degree of graphitization, a higher fraction of fixed carbon (as opposed to volatile carbon) and lower hydrogen to carbon and oxygen to carbon ratios. However, higher processing temperatures result in lower biocarbon yields, so the value of the product must be considered in the context of product yield and energy input.

Hydrothermal carbonization. Biocarbon can also be produced by hydrothermal carbonization (HTC), which is particularly useful for feedstocks with high water content, as this approach avoids the energy-intensive drying process that is typically required before pyrolysis. In HTC, high-moisture-content feedstock is heated under pressure to produce liquid and solid products. The process typically takes place in a closed system in sub-critical conditions and pressure is generated by the reaction products[32]. The solid products are easily recovered, whereas liquid products must be separated from the water. HTC is typically performed at ~180–350 °C (ref. 33). Similarly to pyrolysis, HTC at higher temperatures results in lower hydrogen to carbon and oxygen to carbon ratios in the product owing to dehydration, decarboxylation and condensation reactions that occur simultaneously[32,33]. The elevated pressure and temperature alter the viscosity of water, enabling it to penetrate into the pores of the biomass to assist with degradation[34]. Heating rates and residence time affect product distribution: slower heating rate and longer residence times can improve the extent of carbonization[35].

Other approaches. Other approaches that use alternative energy sources have also been investigated for biocarbon production, such as microwave pyrolysis, plasma pyrolysis, solar thermal and molten salt pyrolysis. Microwave pyrolysis can be advantageous as it allows efficient heating, which can lower residence times[36]. Biocarbon can also be produced using gasification; however, owing to the high selectivity towards gas phase products only low yields of biocarbon are produced. Catalytic pyrolysis is typically used to improve the quality of the liquid product, with biocarbon also produced in this process. Catalysts such as zeolite, alumina and magnesium oxides can be used[37]. In terms of reactor types, continuous reactors can be beneficial for large-scale biocarbon production and reactors such as moving bed, auger, rotating drum and conveyor have shown promise as an alternative to batch processes[38]. Figure 2 summarizes process steps, reactor types and reaction mechanisms involved in pyrolysis of biomass to produce biocarbon.

Mechanism of biomass conversion into biocarbon

Biomass mainly consists of three biopolymers — hemicellulose, cellulose and lignin — which are primarily made with carbon, oxygen and hydrogen. In addition, biomass also contains nitrogen, sulfur and phosphorus, and other inorganic elements to a lesser extent. Hemicellulose, cellulose and lignin have varied decomposition

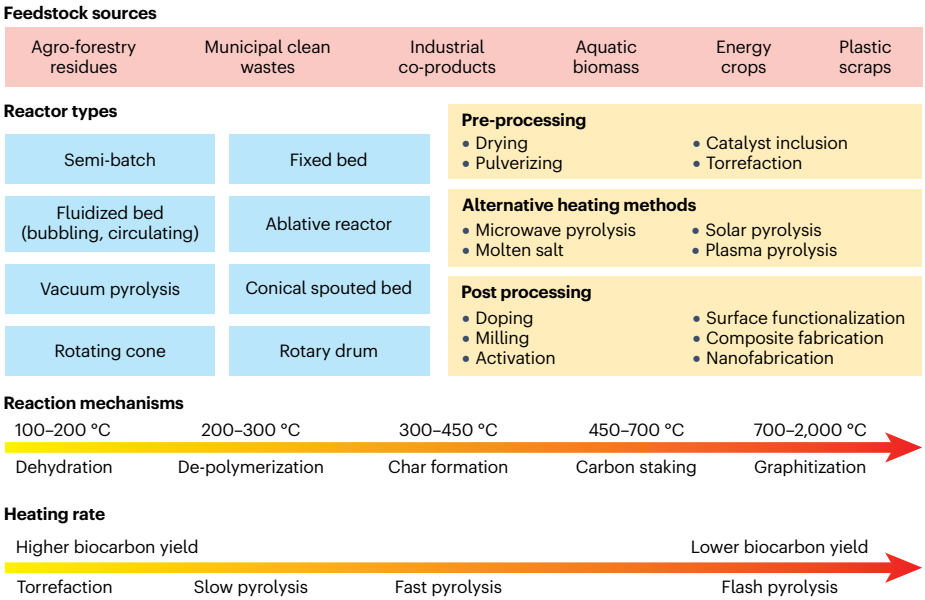

Fig. 2 | Processing methods to produce biocarbon. Pre-processing improves feedstock uniformity and energy density (for example, through torrefaction). Energy can be supplied through combustion or alternative heating methods. Fixed bed reactors offer low cost and high biocarbon yield but have long residence times and challenges in upscaling. Fluidized bed reactors provide good mixing and can be scaled up but have high capital costs and feeding challenges[31]. Fluidized bed reactors may have higher liquid yield (and lower biocarbon yield) than rotary drum reactors. Ablative reactors have efficient heating and higher liquid yields, owing to fast progression of the heat front into the biomass. Rotating cone reactors also produce high liquid yields. Vacuum pyrolysis can operate at lower temperatures owing to lower apparent activation energy[269]. Biocarbon properties can be enhanced through post-processing; activation with CO_2 increases surface area, and functionalities can be added through KOH, H_2O_2 or thermal oxidation treatment. Biocarbon can be incorporated into composite materials or doped with catalytic metals for advanced applications.

mechanisms. Thermal decomposition of hemicellulose and cellulose starts at 200 °C and ~330 °C, respectively, whereas lignin decomposition has a very broad range, starting at ~200 °C with maximum decomposition occurring at >400 °C, owing to its branched structure[39]. During the thermal degradation process, hemicellulose breaks down into anhydro sugars (anhydro xylopyranose), furan and pyran ring derivatives (2-methyl furan and 2-furaldehyde) and low-molecular-weight compounds (CO, CO_2, formic acid and acetic acid)[40]. Cellulose is first transformed into active cellulose, which has a lower degree of polymerization, but without evolution of any volatiles. Active cellulose can be further decomposed by a set of competitive reactions: a slow reaction that produces biocarbon and permanent gases or the main reaction, which produces a tar that contains levoglucosan and other sugars. Lignin is mainly composed of aromatic rings and its decomposition happens over several stages, encompassing a wide temperature range[41]. Thermal decomposition of lignin yields gases, liquids and solid aromatic biocarbon[7]. Primary pyrolysis yields pyrolytic lignin along with low-molecular-weight condensable species (for example, water, carbonyls and alcohols) and permanent gases[41]. Usually, the solid residue of biocarbon has an aromatic and polycyclic structure[42]. Reaction pathways that favour char formation are predominated by intramolecular and intermolecular reorganization, which is also responsible for conferring thermal stability on biocarbon. Depolymerization breaks the bonds in lignin to make small-chain molecules and/or monomers. Also, secondary biocarbon formation is observed and is attributed to inter-pore recombination[39,43,44]. Solid biocarbon is formed through several chemical routes, including dehydration, decarboxylation, aromatization and intramolecular condensation. Based on the pyrolysis temperature, biomass can form turbostratic biocarbon (at lower and moderate temperature) and graphitic biocarbon (at higher temperatures). These mechanisms are influenced by the inorganic content of the biomass[39,45]. The inorganic constituents have a key impact on the pyrolysis mechanisms either by fulfilling a catalytic role (nickel and iron) or by inhibiting certain reactions (silicon and phosphorus)[46,47]. Further studies are needed to understand the complex reaction influenced by these inorganic components to establish efficient catalyst systems for the conversion of biomass into biocarbon with desired properties.

Influence of processing parameters and catalysts

Processing parameters, such as temperature, heating rate, residence time and catalysts can greatly influence biocarbon properties[3]. For example, a review of 72 independent studies reported low average hydrogen to carbon ratios for corn stover (0.25), switch grass (0.18) and wood (0.23), for biocarbon synthesized at higher pyrolysis temperatures (>500 °C)[48]. At lower pyrolysis temperatures (<500 °C), these values increased to 0.60, 0.67 and 0.54, respectively[48]. The same review also reported that biocarbon surface area was 3.8 times higher at pyrolysis temperatures >500 °C, compared with that produced at lower temperatures. Beyond a certain temperature (varies between feedstocks), the surface area starts to decrease owing to pore collapse, pore blocking and fusion as carbonization proceeds[4]. There exists a logarithmic curve to fit the temperature–yield data, shown in Eq. 1 for various types of biomass[49]. In the temperature range 200–300 °C, moisture and labile volatile matter are removed, resulting in a sharp decrease in biocarbon yield (~80% at 200 °C and ~36% at 300 °C).

Between 300 and 700 °C, a continuous decline in yield with temperature is observed, owing to further loss of volatiles. Higher temperatures show less noteworthy changes in yield as many volatiles have already been removed. The structure of biocarbon also changes with temperature: biocarbon produced at low temperatures is primarily composed of amorphous carbon whereas higher temperature leads to more ordered carbon[4]. Studies have confirmed that temperature is the primary factor that contributes to the creation of ordered carbon structure[4]. High temperature (beyond 1,200 °C) is essential for the atomic level orientation or graphitization to occur during carbonization and can be aided by salt-based activation techniques or metal catalysts[50]. Catalytic pyrolysis can help to reduce pyrolysis temperature and increase yield of graphitic biocarbon. The mechanism of carbon dissolution–graphite precipitation is mainly responsible for the graphitization of biomass[51]. High temperature also drastically lowers the number of surface functional groups, mainly aldehyde, ketones and hydroxyls. In biocarbon produced at lower temperatures, there is an abundance of hydroxyl and carboxyl groups, which are helpful in applications such as adsorption of cationic pollutants[52]. High heating rates will also result in lower yield of biocarbon[4]. Increasing residence time during carbonization generally shows similar trends to increasing temperature. For example, increased residence time results in lower yield and higher carbon content, aromaticity, pH and porosity[49,53].

$$\text{Yield (\%)} = -36.25 \ln(\text{temperature (°C)}) + 264.17 \quad (1)$$

(ref. 50).

Modification techniques for biocarbon

Biocarbon modification has become a useful strategy for tuning structural, surface and porosity and functional properties for desired materials, energy and environmental applications. There is a wide range of modification techniques for biocarbon materials, for example, activation, exfoliation, heteroatom doping, oxidative acid treatment, surface modification, composite fabrication and hetero or hybrid structure formation. Detailed information regarding the modification techniques of biocarbon is available in Supplementary information.

Activation. Activation, a technique to increase porosity and surface area, can be categorized as physical (using CO_2, steam, air or ozone), chemical (using KOH, NaOH, K_2CO_3, $ZnCl_2$ or H_3PO_4) and radiation based (using microwave, plasma or γ-irradiation)[54–57]. Chemical activation is widely explored for the biocarbon materials. For example, rubber wood sawdust biocarbon can be activated with KOH through secondary pyrolysis at 800 °C, to increase the surface area[58]. Additionally, the micro and meso pore volumes of biocarbon increase with higher KOH concentrations, from 0.10 and 0.02 $cm^3\ g^{-1}$ to 1.27 and 0.30 $cm^3\ g^{-1}$, respectively. The choice of activation agent also impacts biocarbon yield, with KOH activation yielding more biocarbon than H_2SO_4, H_3PO_4, HNO_3, K_2CO_3 or NaOH for coconut husk carbon[55].

Exfoliation. Exfoliation (separation of the graphitic layers) of biocarbon is achieved through methods such as mechanical, chemical, microwave, ultrasound and liquid-phase exfoliation[59–64] and enhances specific surface area, porosity and surface functional groups[65]. In addition to traditional mechanical and chemical methods, ultrasound-based exfoliation (20 kHz) reveals the layered structure of biocarbon to increase porosity and permeability[66], whereas microwave-assisted exfoliation exposes basal and edge planes[61]. The molten salt-assisted process is another option for biocarbon exfoliation[67]. Similar to conventional graphene, exfoliated biocarbons have the potential to immobilize various active components[68].

Heteroatom doping. Heteroatom doping in biocarbon improves electron transfer efficiency, creates different structural diversities and boosts surface functionality[69]. This process introduces structural defects, increasing surface active sites and functionality in biocarbon, thereby enhancing its performance in applications such as electrochemical energy storage and conversion, catalysis, environmental remediation and CO_2 adsorption. Self-doping[70] involves using nitrogen, phosphorus and/or sulfur-rich biomass as feedstock, whereas external doping[71,72] incorporates targeted elementally rich precursors.

Oxidative acid treatment. Oxidative acid treatment of biocarbon can create surface functionality. Nitric and sulfuric acids can be used to introduce nitro and carboxylic functional groups[73], thereby increasing oxygen content and reducing thermal stability. In the presence of surface functional groups, post-acid treatment can be used to develop polymeric composites with strong interfacial bonding between biocarbon and plastic resin. For example, HNO_3 acid treatment enhances hydrophilicity, pore structure and surface functionalities in nickel–biocarbon[74], and combined H_2SO_4–H_2O_2 treatment can be used to increase the oxygen-containing functional groups in macro-algae-derived biocarbon[75].

Surface modification. Simple chemical reactions can be used to functionalize biocarbon, by incorporating, inorganic, organic, biological and polymeric entities[76]. Furthermore, pyrolysis conditions can be tailored to achieve desired surface mechanical properties in biocarbon. For example, high treatment temperatures (around 900 °C) with a 1 h retention time yield biocarbon with elevated hardness (4.3 GPa) and modulus (25 GPa)[77]. In addition, alkali modifications (KOH and NH_4OH) decrease pore volume and specific surface area[78]. Phosphate and chloride salts alter the surface topography and chemistry of biocarbon[76]. Organic modifications using polymers, organic acids and vitamins create desired surface functional groups and modify surface charge. For example, both chitosan[79] and citric acid[80] modification enhance the oxygen to carbon ratio but reduce the specific surface area of biocarbon. Modifications with vitamins such as vitamin B_6 (ref. 81) and vitamin C (ref. 82) can decrease surface area but enhance aromaticity.

Composite fabrication and hetero or hybrid structure formation. Integration of biocarbon with materials such as metals[83], metal alloys[84], metal oxides[85], chalcogenides[86], hydroxides[87], carbon nanostructures[88], metal carbides[89] and polymers[90] can enhance its physicochemical properties. Biocarbon loaded with silver and silver–copper bimetallic nanoparticles can effectively prevent nanoparticle agglomeration, demonstrating retention of excellent antimicrobial activity[83,91]. Fabrication of metal oxide-based biocarbon composites can create surface active sites with magnetic, photo-catalytic and electrochemical properties[92,93]. For example, introducing metal hydroxide into biocarbon enhances pseudo-type electrochemical active sites[94]. Using biocarbon as a host for metal hydroxides results in a porous architecture, providing a more active surface area. Fabrication of biocarbon–conducting polymer composites facilitates efficient electron transfer through a complex structure, improving the performance[95–97].

Safety considerations

Biocarbon production and handling poses risks, owing to the release of fine particles, especially during fine milling (<10 µm particle size)[98,99]. Although biocarbon particles generally have a larger particle size distribution of biocarbon than other carbon materials, safety protocols must be standardized for processing, transportation and manufacturing. Respiratory protective equipment is advised to minimize exposure risks. Combustion and explosion hazards are also associated with biocarbon dust, especially in enclosed spaces. Particle size reduction increases ignition and combustion rates, potentially leading to flash fires or dust explosions — dust particles <500 µm in size may exhibit explosive characteristics[100]. The settling time of particles varies, ranging from a few seconds for particles approximately 100 µm in size to several hours for particles around 1 µm (ref. 101). Increasing biocarbon density through pelleting and briquetting is recommended to reduce material breakdown and dust formation. Self-heating and self-ignition risks are also associated with biocarbon transport and storage. These risks are higher for biocarbon produced at low temperatures (350–500 °C), owing to the greater amount of volatiles and free radicals on the biocarbon surface[102] so need to be sufficiently moist during transportation. Hazards are reduced for biocarbon produced at higher temperatures (>500–600 °C), owing to their aromaticity and lower volatile content[103]. Free radicals in biocarbon may contribute to self-heating[102]. The impact of inorganic elements and biocarbon ageing on flammability risk needs further understanding. Adjusting biochar moisture content to 20–50% can potentially reduce the flammability risk of biocarbon[104]. Similar recommendations are given by the European Biochar Certificate (EBC).

Results

Biocarbon characterization

Characterization of biocarbon is crucial, owing to variations in feedstock and pyrolysis techniques. Proximate analysis quantifies moisture, volatile matter, fixed carbon and inorganic mineral ash[105]. Elemental composition (carbon, hydrogen, nitrogen and oxygen) of biocarbon is determined by an elemental analyser, with sulfur predominantly found in the mineral ash portion[106]. The volatile matter, mineral ash and moisture content can also be determined using thermogravimetry[107]. Other methods to assess the elemental composition of biocarbon materials include X-ray photoelectron spectroscopy[108], inductively coupled plasma mass spectrometry (ICP-MS or ICP-AES)[109] and scanning electron microscopy (SEM)–energy dispersive X-ray spectroscopy[106]. There are standardized methods used to determine biocarbon moisture content — ASTM D (4442-92) and mineral ash content — ASTM D (1755-95). A widely used method to assess the specific surface area, porosity and pore volume of biocarbon is the Brunauer–Emmett–Teller (BET) method, which uses the surface adsorption of N_2 (at low temperatures) or CO_2 (at relatively higher temperatures). N_2-assisted BET tends to yield lower surface area values than CO_2, which is attributed to limitations related to the kinetics of N_2 diffusion into micropores, owing to the effective diameter[53]. Biocarbon particle density, usually determined by pycnometer, typically ranges between 1.5 and 2 g cm^{-3} (ref. 110). Particle size distribution of biocarbon can be easily determined using stacked sieves with different opening sizes[111]. Alternative methods to analyse biocarbon size include laser diffraction, investigating the intensity variation of scattered laser beam[112], electron microscopy or using software such as ImageJ to analyse photographic images[113].

The morphology and topography of biocarbon can be visualized using SEM[114]. SEM coupled with energy dispersive spectroscopy can also reveal the elemental composition of biocarbon. Transmission electron microscopy (TEM) and aberration-corrected TEM are used to analyse nanoscale features of biocarbon, for example, the arrangement of carbon atoms, and thermogravimetric analysis can be used to determine the thermal decomposition profile of biocarbon[115]. Phase purity and crystallinity of biocarbon can be revealed by X-ray diffraction. Fourier transform infrared spectroscopy can be used to analyse chemical make-up of biocarbons[116], and Raman spectroscopy can determine the in-plane crystallite size distribution[117]. Solid-state NMR spectroscopy can be used to evaluate the presence of aromatic and aliphatic hydrocarbons in biocarbon[118], chemical structure, long-term stability and the mechanism involved in biocarbon formation. Nanoindentation measures the hardness of biocarbons as the ratio of maximum load to contact area (Box 1). Cone calorimeter tests of biocarbon provide information on its reaction-to-fire properties. Electrical conductivity is assessed through alternating current (AC) or direct current (DC) methods.

Techno-economic and life-cycle assessment

The feasibility of biocarbon use on a large scale hinges not only on its technical performance but also on the economic viability and environmental impact of production projects. Techno-economic assessment (TEA) and life-cycle assessment (LCA) are crucial to identify cost-effective and environmentally sustainable methods[119,120] and may include various stages of the biocarbon life cycle, as presented in Fig. 3. TEA evaluates costs, risks and uncertainties throughout the production and application system[121], considering parameters such as feedstock production and transportation costs, facility expenses and project revenues across various stages of the production chain. Sensitivity and risk analyses can identify the parameters that impact the economic viability of a project. The minimum selling price, crucial for commercial-scale biocarbon applications, denotes the selling price required to attain a net present value of zero within a specific project (economic feasibility). The minimum selling price of biocarbon varies widely — US$200–2,000 per ton[122–124] and as high as approximately $18,000 per ton for virgin wood feedstock biochar[125] — based on specific characteristics and production process conditions. This price variability may be explained by the wide biocarbon quality ranges, which is related to physical and chemical characteristics, and the multiplicity of potential uses. Despite challenges in direct comparison with fossil-based equivalent materials, studies reveal competitive biocarbon production costs, particularly when integrated with other processes such as bioenergy or biofuel production[126,127]. A comprehensive biorefinery approach, to generate valuable products from bio-oils and syngas to maximize the economic and environmental benefits of biomass and waste conversion, may be a promising strategy for a more sustainable and efficient bio-based economy[128]. Carbon removal certificates or carbon credits may further enhance the economic feasibility of biocarbon initiatives[123].

LCA is essential for informed decision-making in the development of sustainable production strategies of biocarbon and biorefinery projects, adhering to ISO 14040 and ISO 14044 standards. The global warming impact, expressed in CO_2eq, is the typical metric for comparing processes or products. The potential of biocarbon to reduce greenhouse gas emissions is a widely acknowledged benefit[129–132]. LCA results are influenced by biocarbon production conditions such as pyrolysis temperature and residence time[121] as well as by feedstock supply considerations related to land use, fertilizer application and transport emissions[130]. Utilizing residual biomass and waste in a circular economy approach may represent a sustainable and cost-efficient resource for biocarbon production. TEA and LCA are valuable tools

Box 1

Determining the inherent mechanical properties of biocarbon

The typically small and irregular size of biocarbon makes it difficult for conventional techniques to determine its innate mechanical properties. Alternative methods such as Vickers hardness test, nanoindentation and atomic force microscopy are used to discern these properties. All hardness tests measure pressure as force over area, requiring sample thickness to be at least five times that of the indenter penetration depth.

Vickers hardness test

The Vickers hardness test is suitable for biocarbon particulates in the micrometre range. Biocarbon particulates are embedded in epoxy resin, cured, ground and polished before undergoing the Vickers hardness test. A known load is applied through a pyramidal diamond indenter and the resulting indent surface area is measured to obtain the hardness value (HV) according to the formulae:

$HV = \frac{1.85F}{d^2}$, when HV is in kgf mm^{-2} and $HV = \frac{0.189F}{d^2}$, when HV is in MPa.

Where F=force applied and d=average diagonal length of the indenter's impression on the tested sample (mm).

Nanoindentation

For biocarbon particulates in the higher Ångstrom, nanometre and sub-micrometre range, the nanoindentation test can be used[282]. In comparison to the Vickers test, nanoindentation uses a much lower load and smaller indenter (Berkovich). The indenter tip is applied with a set maximum load and/or displacement, followed by reducing the load to zero. Mechanical properties such as hardness and modulus are determined using the Oliver and Pharr method for nanoindentation[283]. Nanoindentation is often paired with scanning probe microscopy to image the indentation effect.

Atomic force microscopy

For biocarbon particulates in the Ångstrom range, an atomic force microscope can be modified by attaching a three-sided pyramidal diamond indenter. Similar to other hardness tests, nano-hardness is determined by dividing the applied load by the residual area on the sample[284]. This test is particularly useful for ultra-small biocarbon particulates and polymer thin films that contain biocarbon.

for research and engineering communities to identify and prioritize pathways for process development and optimization, for investors to assess project revenues and profitability indicators and for policymakers to identify incentives and regulations to support the development of emerging technologies.

Applications

Polymer composites

Researchers have explored the development of biocarbon-added composites using different polymeric resins for various applications[133–135]. However, the specific characteristics of biocarbon that are crucial for performance properties in a given composite remain unclear.

The hardness and stiffness of biocarbon can be determined through techniques such as nanoindentation[136], Vickers hardness test and atomic force microscopy. Usually, both hardness and stiffness of biocarbon increase with pyrolysis temperature up to 1,000 °C (refs. 137,138), owing to the development of a crosslinked structure with strong intermolecular forces and C–C covalent bonds. Beyond this temperature, a decline in hardness and stiffness occurs, owing to crosslink bond breakages and basal plane slippage (during indentation) of graphitic carbons[139,140]. To achieve high hardness and stiffness in biocarbon-added composites, a pyrolysis temperature range of 700–1,000 °C is recommended. For example, biocarbon from pine wood pyrolysed at 900 °C increased Young's modulus in polypropylene composites, compared with biocarbon pyrolysed at 350 °C (ref. 141).

Similar effects are observed in biocarbon composites with thermosetting plastics[142] and elastomers as the matrix[143] when pyrolysed at 800 °C, indicating the potential to enhance the stiffness in biocarbon composites around this temperature.

The porosity and surface area of biocarbon are influenced by pyrolysis temperature, with pores developing between 300 °C and ~400–600 °C. BET surface adsorption of N_2 and CO_2 can be used to determine biocarbon porosity[144]. Biocarbon typically has three pore types – macropores (0.05–1,000 µm), mesopores (0.002–0.05 µm) and micropores (0.0001–0.05 µm). Polymer–biocarbon interaction depends on pore volume; polymer flow through the macro and mesopores of biocarbon during processing creates mechanical interlocking, reduces polymeric chain mobility and increases stiffness. For example, when added to high-density polyethylene composites[145], rice husk-derived biocarbon (pyrolysed at 600 °C) showed increased surface area and pore volume compared with the untreated biocarbon, enhancing flexural strength and modulus. Activation improved polymer flow through the porous structure of activated biocarbon, compared with the non-activated biocarbon[145]. The type of feedstock also influences porosity: wood apple fruit shell biocarbon (pyrolysed at 800 °C) had higher macro porosity than pigeon pea-derived biocarbon[142]. Furthermore, the porosity of palm kernel shell-derived biocarbon enhanced the physical interaction with carboxylated nitrile butadiene rubber, increasing hardness in the rubber composites[146]. In general, the porous nature of biocarbon can facilitate greater interaction with polymeric resins.

The surface functionality of biocarbon, attributed to chemical functional groups, diminishes at higher pyrolysis temperatures (500–750 °C) when these groups are removed[144,147]. Infrared spectroscopy is used to analyse surface functionality; surface functionality and porosity of biocarbon have an inverse relationship whereby surface functionality decreases and porosity increases at high pyrolysis temperature. Low-temperature biocarbon (<400–500 °C) with aldehyde, hydroxyl and ketone-based functional groups interacts well with polar resins, whereas high-temperature biocarbon (>500 °C) has better interaction with non-polar resins, owing to reduced surface functionality. In the latter case, the interaction is porosity dependent.

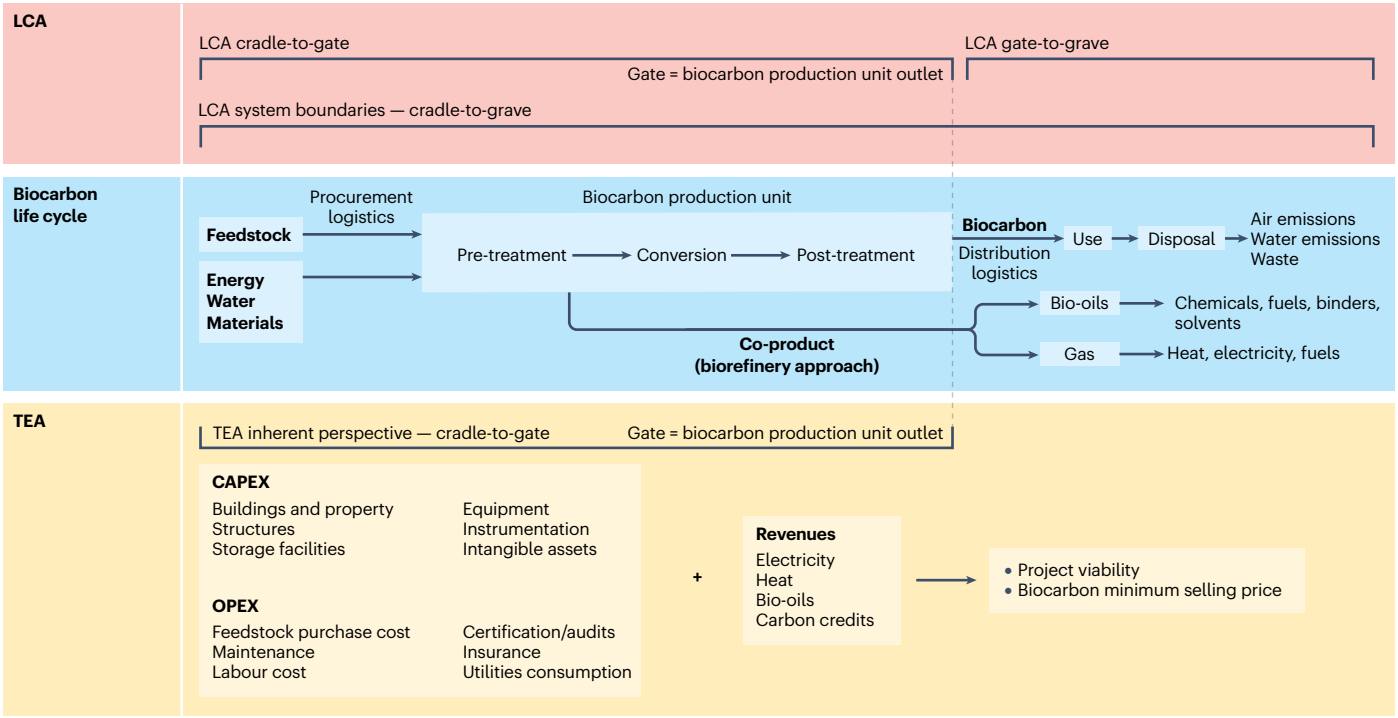

Fig. 3 | Techno-economic and environmental assessment approaches for biocarbon evaluation. The biocarbon life cycle includes all stages from feedstock extraction or collection to use and disposal. Techno-economic assessment (TEA) and environmental assessment of biocarbon can include all or selected stages of biocarbon life[270]: the cradle-to-grave approach is used in a typical life-cycle assessment (LCA) approach. Stakeholder objectives may dictate other system boundaries such as cradle-to-gate, gate-to-grave or cradle-to-cradle. For biocarbon engineering, a cradle-to-gate approach can help to identify sustainable feedstocks and conversion processes. Gate-to-grave assesses environmental performance of different biocarbon and disposal alternatives. Cradle-to-cradle interrogates biocarbon in a circular economy. TEAs typically use cradle-to-gate boundaries, considering feedstock production transportation costs, facility costs and project revenues, to ensure economic viability on a commercial scale[271]. Production conditions, such as pyrolysis temperature and residence time, feedstock composition and biocarbon physicochemical properties impact the TEA of biocarbon.

At low pyrolysis temperature, some volatiles may remain clogged in the pores (see Supplementary information) and aid the ignition of biocarbons[148,149]. For fire safety, highly carbonized biocarbon with no surface functionality and strong C–C covalent bonding is preferred. This thermal stability enables the use of biocarbons with engineering plastics at high processing temperatures, unlike plastics that have ligno-cellulosic natural fibre counterparts, which start decomposing at 200 °C.

Biocarbon particle size impacts dispersion and wetting. Size can be controlled using milling, grinding and sieving and size distribution can be determined by the laser diffraction method. Numerous studies have been conducted to determine the effect of biocarbon particle size on polymeric composites[150–152]. Generally, reducing particle size by milling eliminates micropores, increases the specific surface area and heat deflection temperature, strengthening the composite (both tensile and flexural)[153]. For example, smaller particle size (20–75 µm) improved tensile and flexural strength of thermoplastic composites compared with larger particles (~150–300 µm)[151]. For epoxy composites, a particle size of 80 µm increased the tensile, flexural and impact strength compared with the neat epoxy and the composites without any biocarbon[154]. Biocarbon particles with a size below 10 µm, co-milled with nano-silica, enhanced mechanical properties in carbon black-replaced styrene butadiene rubber composites[155].

Biocarbon loading amount in composites is important, because above a certain point, particle agglomeration occurs, which is detrimental to mechanical properties. Optimal amounts of biocarbon vary by material type: 20–25 wt% for thermoplastic composites[141,156,157], <10 wt% for thermosetting plastics[142,154,158] and 25–50% (of the filler) for elastomer composites[159–161]. In additive manufacturing, a very low loading amount of 1 wt% is optimal, regardless of the resin used (see Supplementary information)[162–164]. Increased biocarbon loading results in a more viscous polymer mixture, necessitating higher processing temperatures. For toughened polypropylene with an elastomeric phase (for example, poly(octane ethylene) copolymer), appropriate loading and compatibilizer enhance the interfacial interaction of biocarbon with the resin (Fig. 4). This occurs by reducing the extent of encapsulation of the biocarbon particles by the copolymer[165,166]. Homogeneous mixtures of biocarbon in thermosetting plastics can be obtained by extensive mixing to eliminate void formation (Fig. 5).

Despite the advantages in polymeric composites, biocarbon is not a universal solution for all the materials research challenges. Typically derived from waste biomass or plastic scraps, the small (micrometre-scale) and irregular particle size limit the ability of biocarbon to replace high-aspect-ratio fibre (both natural and synthetic) in polymeric composites. Biocarbon can only replace or supplement particulate reinforcements (for example, talc and carbon black)

and short fibres (for example, short glass fibres). Studies replacing talc (30 wt%) with biocarbon in polypropylene-based composites showed improved flexural strength and similar tensile strength, with reduced environmental impacts, compared with the control sample[167,168]. Adding biocarbons to E-glass fibres in a vinyl ester resin-based composite enhanced the tensile and flexural strength[169]. Careful consideration of the type and constituents of contemporary polymeric composite is essential to optimize biocarbon use for enhanced performance properties and sustainability.

Energy storage

Growing energy demands have driven the development of a wide range of energy storage and conversion technologies, which seek high performance, cost effectiveness and sustainable materials[170].

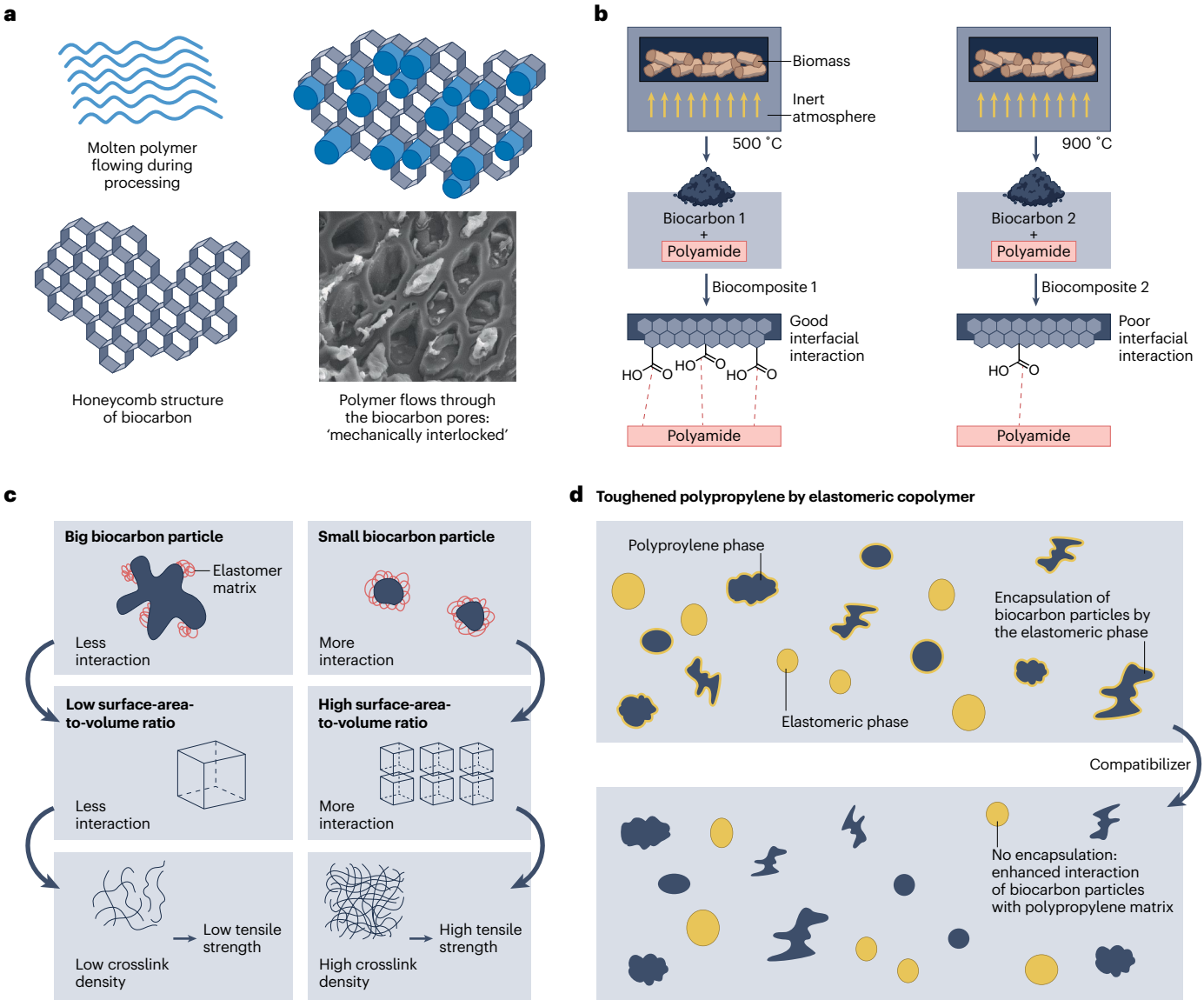

Fig. 4 | An overview of the various types of interaction of biocarbon in polymeric composites. a, Physical interaction of biocarbon in composites: high-temperature biocarbon (500–900 °C), with its porous structure facilitates a mechanical interlock with molten or softened polymer that flows through the honeycomb structure[136]. This interaction, predominant in polymeric resins, including thermoplastics and thermosets[272–274], increases the modulus and flexural strength of the resulting composites[275]. **b**, Biocarbon in polyamide-based composites: biocarbon produced at low temperatures with specific functional groups is more effective at interacting with polyamide- or nylon-based composites. Hence, high-temperature biocarbon may exhibit inferior interfacial adhesion for nylon composites[152]. **c**, Biocarbon in elastomeric composites: smaller particle size can improve biocarbon properties, such as tensile strength, in elastomeric composites[155]. The greater surface-area-to-volume ratio (compared with bigger counterparts) can enhance interaction with the elastomeric matrix, resulting in high crosslink density and tensile strength. **d**, Biocarbon in toughened polypropylene composites: in toughened polypropylene composites that contain biocarbon, the elastomeric phase encapsulates the biocarbon particulates and hinders the interaction with the polypropylene matrix. However, the use of a compatibilizer, such as maleic anhydride grafter polypropylene, can alleviate this issue, enabling direct interaction between biocarbon and the polypropylene matrix[165,166].

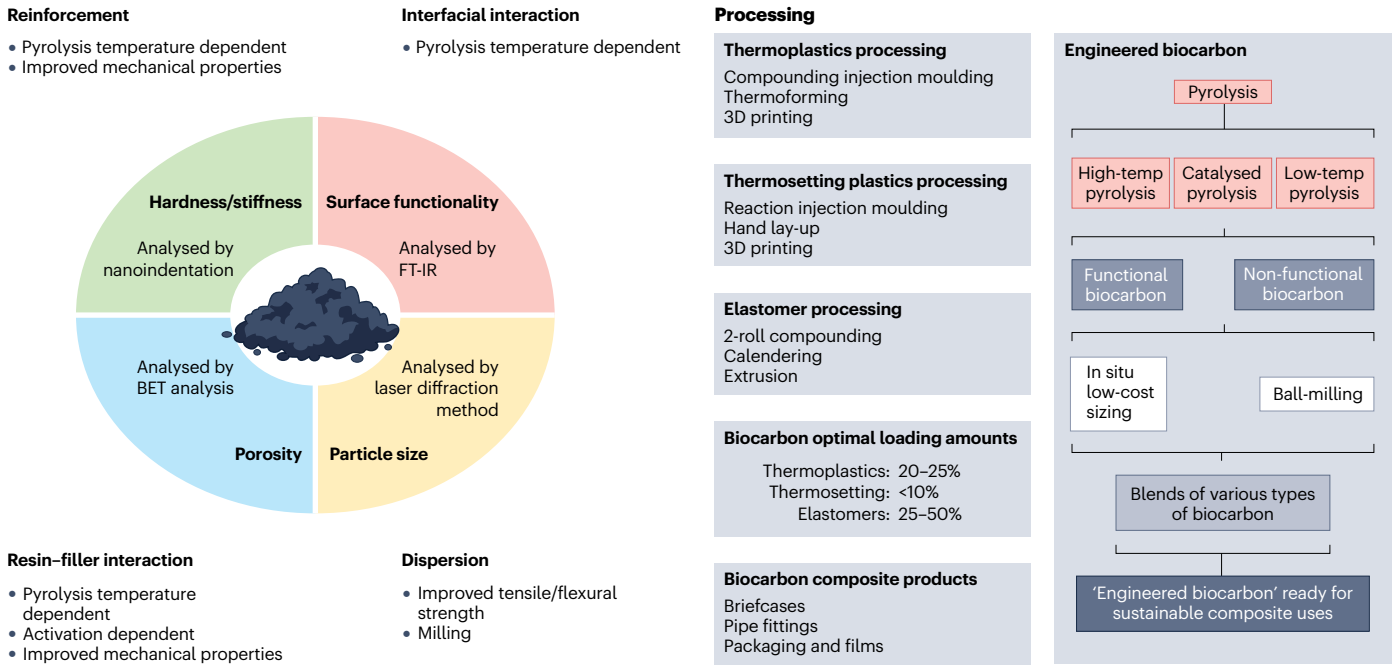

Fig. 5 | A schematic overview of composite applications of biocarbon. Key properties of biocarbon crucial for composite applications include hardness and stiffness, porosity, surface functionality, particle size and loading amount. Hardness and stiffness of biocarbon, determined through nanoindentation, increases up to around 1,000 °C, reinforcing polymeric composites. Porosity and surface area increase up to 800–900 °C and are analysed using techniques such as Brunauer–Emmett–Teller (BET) for surface adsorption of N_2 and CO_2. Surface functionality from chemical functional groups, analysed using techniques such as Fourier transform infrared spectroscopy (FT-IR), is higher at lower pyrolysis temperatures (<500 °C), at which polar polymers have a better interfacial interaction with polar functional groups. Non-polar polymers favour high-temperature biocarbon through a porosity-driven mechanism. Smaller particle size, controlled by milling and sieving, can improve composite strength. Particle size distribution can be determined by techniques such as laser diffraction and ImageJ analysis. Biocarbon-added composites, processed through conventional techniques, yield marketable products with applications such as hardware cases, pipes, insulation panels, packaging and films. Engineering biocarbon for specific applications involves pyrolysation in specialized reactors, controlling size and adopting effective hybridization strategies. The application of biocarbon in composites contributes to waste reduction, material circularity and functional properties such as conductivity, fire safety (see Supplementary Fig. 1) and electromagnetic shielding.

Carbon allotropes, produced from various fossil feedstocks, are the most versatile for various energy storage and conversion technologies. Biomass enables the formation of various carbon structures such as carbon dots, carbon nanotubes, carbon nanofibres, graphene structures, graphitic carbons, activated carbon and turbostratic carbon structures, which are useful for diverse energy storage and conversion applications[12,13,171,172]. Biocarbons have unique physicochemical properties such as hierarchical porous structure, surface functionality and electrical conductivity, which are essential for efficient energy storage and conversion.

Hydrogen storage. Hydrogen is widely used in transportation and electricity production[173], with an increased focus on green-hydrogen production (through electrolysis, photosplitting and thermolysis of water), storage and transportation[174]. Hydrogen storage in biocarbon at room temperature is facilitated by the high specific surface area, high oxygen content and acidic surface groups. Hydrogen storage mechanisms involve physisorption (adsorption of hydrogen molecules at the surface of the material) and chemisorption (the hydrogen is stored by means of chemical reaction). Physisorption utilizes van der Waals force to capture hydrogen and can be achieved in pristine biocarbon without surface modification[175]. Chemisorption involves stronger bonds (covalent) and interaction with the carbon atoms at the surface. Chemisorption is generated by surface modification through doping with chemicals such as alkali hydroxides, alkali carbonates, metals and hydrides. Biocarbons from renewable resources such as wood chips[176], poplar sawdust[177], almond shell[178] and coffee waste[179] have been used for hydrogen storage.

Batteries. Biocarbons, with their inherent properties of hierarchical 3D pore structure, high specific surface area and larger pore volume, offer desirable features for battery electrode materials by minimizing diffusion pathways and ion transport resistance. Lithium-ion batteries, favoured for their high energy density, use carbon (graphite), lithium metal, metal alloys and transition metal oxides as the anode against transition metal-based intercalating components as cathode ($LiCO_2$, $LiMn_2O_4$, $LiFePO_4$) to achieve balanced specific energy and power density[10]. Despite the superior energy storage of lithium metal, its high reactivity limits the overall lifespan[180], prompting research into carbon allotropes as the anode material for lithium-ion batteries[181]. Biocarbons from sources such as coir pith[182], cashew nut sheath[183] and cotton stalk[184] serve as sustainable alternatives to conventional graphite[171]. The development of sodium-ion batteries to replace lithium-ion batteries has generated scientific interest,

owing to the abundance of sodium and its comparable electrochemical behaviour to lithium[185]. Engineered carbon materials with larger interlayer spacing have been explored as anodes to accommodate Na^+ ion intercalation (insertion and de-insertion) in sodium-ion batteries[186].

Metal–air batteries, including zinc–air, lithium–air, aluminium–air and magnesium–air, show high energy density, making them suitable for many applications[187]. Both oxygen reduction and evolution reactions are the key factors in metal–air battery systems. The efficiency of these batteries relies on the catalytic performance of electrodes. Biocarbon derived from peanut shells[188], mushroom[189], exfoliated biochar[190] and loofah[191] have been widely used as electrode materials, owing to their effective ORR performance[192]. Notably, biocarbons with rich nitrogen content have superior performance in metal–air batteries[193].

Supercapacitors. Supercapacitors, renowned for high-power density, fast charging, thermal stability and larger cycling performance, can be classified as electrical double layer capacitors (EDLCs), pseudocapacitors and hybrid capacitors[9]. Biocarbon with higher electrical conductivity, surface functionality and microporous structure exhibits superior capacitive performance, which can be further improved by post modification[54,194]. Biocarbon materials derived from a range of biomass such as switch grass[195], lignin[196], distiller's dried grains with solubles (DDGS)[71], fungal biomass[197] and seaweed[198], show potential as electrode materials for supercapacitors. Biocarbons have also been explored as the active electrode material for zinc-, lithium- and sodium-ion capacitors[199–201]. Table 1 shows the impact of various modification techniques on the biocarbons derived from lignin for energy storage applications. Graphitized biocarbons, produced through high-temperature catalytic pyrolysis, exhibit electrical conductivity comparable to that of commercial conducting carbon[202–204]. The synthesis mechanism for graphitic biocarbon through catalytic pyrolysis is illustrated in Fig. 6.

Energy conversion

Fuel cells. Conductive biocarbons sourced from renewable resources have been successfully used in fuel cells as sustainable alternatives to conventional materials[205,206]. In proton exchange membrane fuel cells (PEMFCs), biocarbon, doped with nitrogen, sulfur and phosphorus, serves as a cathodic ORR catalyst, replacing platinum and its alloys. Metal–nitrogen–carbon materials, as a substitute for noble metals, are another class of catalyst for ORR[207,208]. In direct carbon fuel cells (DCFCs), the disordered lattice structure, poor crystallinity, surface defects, functional groups and electrical conductivity of biocarbon enhance its reactivity with molten carbonate electrolytes compared with conventional carbon materials[172]. A balance between poor lattice structure and electrical conductivity can improve the performance of DCFCs. In microbial fuel cells (MFCs)[12] biocarbons effectively act as the cathodic catalyst, owing to their excellent ORR activity and potential substitution for granular activated carbon. MFCs offer dual benefits of energy generation and wastewater treatment with economic advantages[12].

Solar energy conversion. The limitations of first- and second-generation solar cells, such as manufacturing costs and limited availability of rare elements, prompted the development of third-generation solar cells[209]. In dye-sensitized solar cells, various carbon materials, including biocarbons, have been explored as sustainable alternatives to conventional metal-based components such as sensitizers, photoanodes and counter-electrodes[13]. Biocarbons, in their pristine and composite forms, have been extensively used as sensitizers[210], additives for photoanodes[211] and counter-electrodes[212]. They have a vital role in enhancing cell characteristics, providing environmental and economic benefits compared with conventional materials[213].

Hydrogen production. Conventional hydrogen production is unsustainable and energy consuming, leading to a growing focus on bio-hydrogen production. Carbon materials from various types

Table 1 | Capacitive performances of lignin-derived biocarbon materials with structural and morphological diversity

Structural and morphological feature	Synthetic conditions	Specific surface area ($m^2 g^{-1}$)	Electrolyte	Specific capacity	Ref.
Activated carbon	KOH-mediated microwave activation (800 W, 30 min)	3,065	6 M KOH	325 $F g^{-1}$ @ 0.5 $A g^{-1}$ (3 electrode)	260
Activated electrospun carbon fibres	H_3PO_4 activation (900 °C)	2,340	1 M H_2SO_4	48 $F g^{-1}$ @ 2 $A g^{-1}$ (2 electrode)	261
Carbon nanofibre mats with MnO_2 nanowhiskers	MnO_2 deposition over electrospun carbon fibres (1,200 °C)	583	1.0 M $LiPF_6$	83 $F g^{-1}$ (2 electrode)	262
Nitrogen-doped porous carbon	Hydrothermal carbonization–KOH activation, adenine nitrogen source (850 °C)	2,957	1 M KOH	372 $F g^{-1}$ @ 1 $A g^{-1}$ (3 electrode)	263
Nitrogen–sulfur-doped porous carbon	Lignin amine and Fe_3O_4 template (700 °C)	1,199	6 M KOH	241 $F g^{-1}$ @ 1 $A g^{-1}$ (3 electrode)	264
3D interconnected porous structures	Green bacterial activation (900 °C)	1,831	6 M KOH	428 $F g^{-1}$ @ 1 $A g^{-1}$ (3 electrode)	265
NiO nanoparticles in mesoporous carbons	Wet chemical synthesis with $Ni(NO_3)_2 \cdot 6H_2O$ (600 °C)	802	6 M KOH	880 $F g^{-1}$ @ 1 $A g^{-1}$ (3 electrode)	266
Hierarchical porous carbon aerogels	Sol-gel, ambient drying followed by pyrolysis at 1,050 °C then KOH activation (800 °C)	779	6 M KOH	143 $F g^{-1}$ @ 0.5 $A g^{-1}$ (3 electrode)	267
Carbon nanospheres	Self-assembly, stabilization treatment	736	6 M KOH	147 $F g^{-1}$ @ 0.5 $A g^{-1}$ (3 electrode)	268

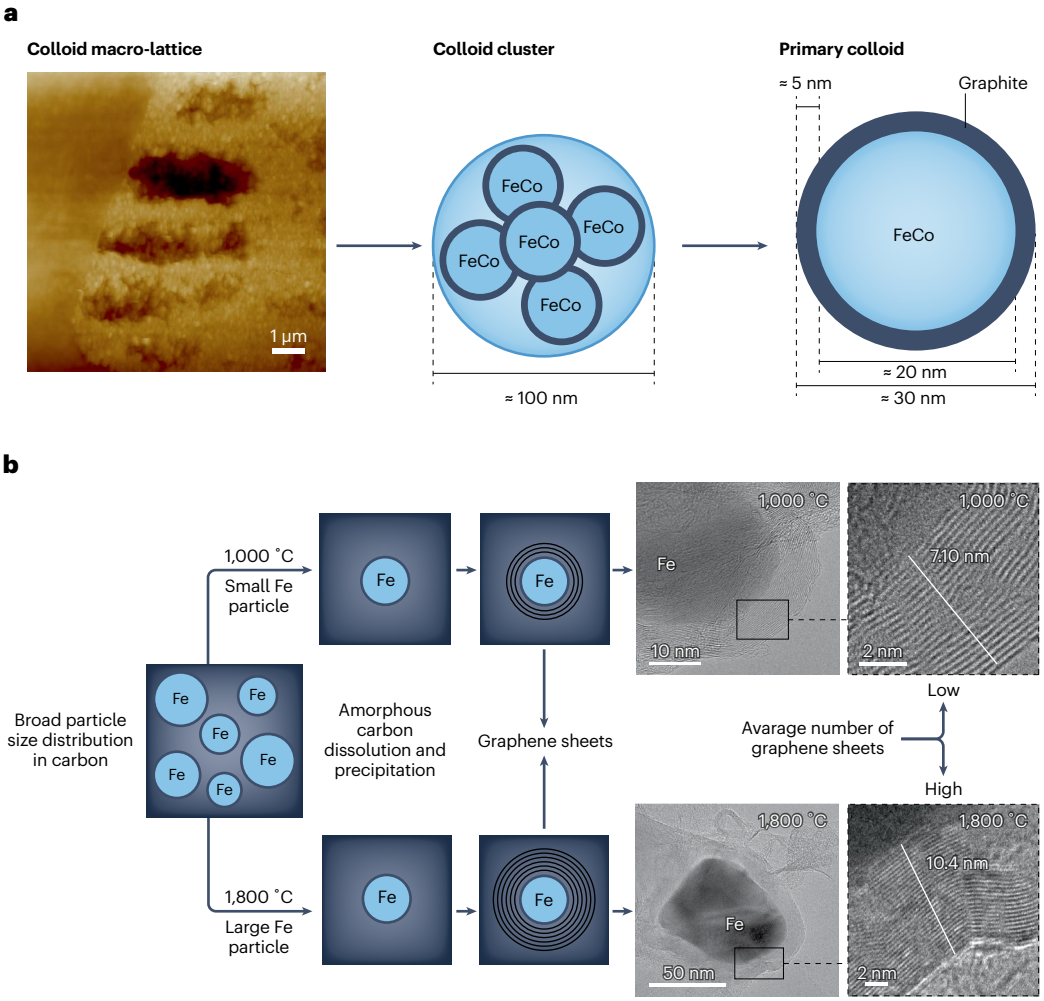

Fig. 6 | Catalytic production of graphitic biocarbon and its application in energy storage devices. a, The idealized model, which suggests the fractal assembly of graphitized biocarbon grown over the surface of FeCo catalyst[202]. **b**, Schematic representation of the mechanism involved in the graphitization of cellulose-derived biocarbon and the impact of pyrolysis temperature and catalytic particle size on the average number of graphene sheets along with the high-resolution transmission electron microscopy (HR-TEM) images of graphitic biocarbon pyrolysed at 1,000 or 1,800 °C (ref. 51). Such catalytic pyrolysis can be used to produce biographene from various sustainable and renewable resources[276]. Part **a** adapted with permission from ref. 202, Royal Society of Chemistry. Part **b** adapted with permission from ref. 51, Wiley.

of biomass, with their porosity, high specific surface area and electrical conductivity, serve as precursors to enhance bio-hydrogen production[214]. Bio-hydrogen can be produced from biocarbons by methane steam reforming, water splitting and anaerobic digestion[215]. Biocarbon has an important role in electron transmission during the hydrogen fermentation process; improving extracellular electron transfer promotes fermentation for hydrogen production[216]. Nitrogen doping in biocarbons increases electrical conductivity and promotes fermentation for higher hydrogen yield[214]. The pyrolysis temperature of biocarbon influences the concentration of dissolved organic matter in the fermentation reactor, impacting H_2 accumulation[217].

Environmental remediation

Wastewater treatment. Biocarbon proves effective in wastewater treatment by removing pollutants that have been addressed historically, such as organics, dyes, metals and nutrients, as well as emerging pollutants such as pharmaceuticals. Various post-pyrolysis modifications are used, such as chemical or physical activation to enhance the specific surface area, acid treatment (for example, HNO_3 or H_2SO_4) to increase the hydrophilic nature, alkali treatment (for example, NaOH) to enhance adsorption capacity and metal or heteroatom doping, which further improves metal ion removal[218]. Biocarbon effectively removes heavy metals such as As^{3+}, Cr^{3+}, Cr^{6+}, Cd^{2+}, Cu^{2+} Zn^{2+} and Pb^{2+} (ref. 36), via various reaction mechanisms including ion exchange[219] with inorganic components within the biocarbon. Mechanisms are influenced by properties such as aromatic functional groups, surface charge, pH and stability[220].

Biocarbon exhibits effective wastewater treatment by adsorbing organic pollutants such as phenol, dyes (malachite green, methylene blue, crystal violet, Congo red and orange G)[219] and pharmaceuticals (tetracyline, sulfamethoxazole, diclofenac and ofloxacin)[221]. Reaction mechanisms for pharmaceutical removal vary, including electrostatic,

hydrophobic, π–π interactions, hydrogen bonding, functional group complexation, pore filling and ion exchange[221] as shown in Fig. 7. It is important to match the chemical properties of the biocarbon surface to the electrostatic properties of the targeted contaminant. Biocarbon application in wastewater treatment can also enhance flocculation, dewatering, adsorption and oxidation[2].

Biocarbon has been used for the removal of microplastics from water, with adsorption of both pristine and aged polyamide microplastics recently demonstrated[222]. Attributed to complexation, hydrophobic interaction and electrostatic interaction, removal efficiencies of 97% were achieved for aged polyamide microplastics under optimal neutral pH conditions. Notably, smaller particle size enhanced removal efficiency, highlighting the importance of the biocarbon pore structure. Biocarbon used in oil spill clean-up has been shown to outperform activated carbon in kinetics and sorption capacity[223,224]. In oil spill clean-up, biocarbon undergoes functionalization to enhance hydrophobicity[225,226], which improves adsorption and minimizes water uptake in pores, leaving greater surface area for organic compound removal[227]. Magnetic biocarbon could facilitate spent sorbent recovery in oil spill clean-up.

CO_2 adsorption. Biocarbon has potential applications in carbon capture and storage (CCS), CO_2 direct air capture (DAC) and air quality improvement. Advantages over conventional materials include renewability and sustainability. However, the CO_2 uptake of biocarbons is influenced by morphology, structure and surface chemistry. Biocarbon preparation, often involving activation or doping methods, should be adapted for this application to develop the required pore structure and surface composition[228]. Pristine biocarbons exhibit limited CO_2 adsorption compared with engineered biocarbon materials (such as activated carbons and graphitic biocarbons), as observed in studies with pyrolysed coffee grounds[229], agricultural residues and wood[230].

A well-developed micropore volume, particularly in the range below 0.8 nm at atmospheric pressure and below 0.5 nm at subatmospheric pressure, is important to enhance CO_2 adsorption[231]. High surface areas or large total pore volumes do not necessarily correlate with high CO_2 uptake[231]. The volume of narrow micropores is key for increased CO_2 adsorption, suggesting a pore-filling mechanism. Both a homogeneous ultra-microporous structure[232] and surface chemical composition have key roles in CO_2 capture[233]. By optimizing the activation method, carbon adsorbents can be prepared with controlled structure and chemical composition. For example, relatively high-uptake capacities are reported for KOH-activated carbon from bamboo, going up to 3.5 mmol CO_2 per gram (25 °C and 1 bar)[234] and chemically activated carbons from palm stones using various activating agents ($ZnCl_2$ and H_3PO_3) showed similar uptake capacities of 3.9 mmol CO_2 per gram and 4.16 mmol CO_2 per gram, respectively (0 °C and 1 bar)[235]. Nitrogen doping also results in improved adsorption, owing to the increased interaction between CO_2 and the carbon surface. However, further research is still required to optimize the CO_2 capture capabilities under more representative conditions and to assess biocarbon reusability in the production methods.

Other applications

Sensors. Biocarbons with modified structures serve as effective sensing materials for various environmental and physical parameters, owing to their effective electron transfer capabilities[236]. Derived from various types of biomass, porous biocarbons have been used as

a

Pollutants		Mechanisms involved
Heavy metals		
As^{3+} Cr^{3+} Cr^{6+} Cd^{2+}	Cu^{2+} Pb^{2+} Zn^{2+}	Ion exchange Electrostatic attraction Coprecipitation
Organics and dyes		
Phenol Methylene blue Malachite green Crystal violet	Orange G Congo red	Pore filling Van der Waals forces n–π interaction Dipole–dipole
Pharmaceuticals		
Sulfamethoxazole Ofloxacin Acetaminophen Tetracycline	Guarylurea Diclofenac	Pore filling Hydrophobic interaction Electrostatic interation n–π interaction π–π interaction

b

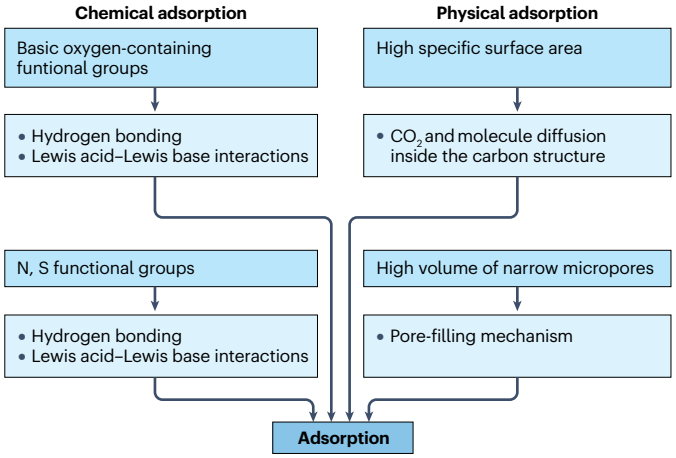

Fig. 7 | Mechanisms involved in adsorption of pollutants by biocarbon. **a**, Adsorption mechanisms for compounds that can be removed from wastewater using biocarbon. Heavy metals are removed through mechanisms such as physical adsorption, electrostatic attraction, ion exchange and complexation[277]. Surface modifications, such as surface oxidation, can improve performance by adding functional groups that can interact with pollutants. Mechanisms for pharmaceutical removal include hydrogen bonding, n–π interactions and van der Waals forces. The morphological properties of biocarbon influence pore-filling mechanisms, which require larger pores for removal of bulkier compounds[278]. Organic compounds and dyes can interact with biocarbon by pore filling, electrostatic interactions and ion exchange capacity. Pollutants that contain benzene rings can interact with biocarbon via π–π electron donor interactions, which are more available with increasing oxygen functional groups on the biocarbon surface[279]. **b**, Mechanisms involved in CO_2 adsorption by biocarbon. The CO_2 uptake abilities of biocarbons depend on structure and surface chemistry. Adsorption primarily occurs via physical adsorption through a pore-filling mechanism in well-developed micropores. Narrow micropores (~0.33–1 nm) show significant effectiveness on CO_2 adsorption[280]. Smaller pores are not suitable for this application, owing to the kinetic diameter of the CO_2 molecule (0.33 nm). Chemical adsorption mechanisms also have a role; for example, nitrogen doping can enhance CO_2 uptake abilities of biocarbons. Sulfur dopants may generate strains and defects in the carbon matrix, increasing local reactivity. Strong acid–base interactions between CO_2 and C–S functionalities could play a predominant part in CO_2 adsorption[281].

electrochemical sensors to detect food contaminants, pharmaceuticals, organic pollutants, metal ions and biomolecules. Carbon dots derived from various types of biomass are being used as colorimetric and fluorometric sensors to remove various metallic contaminants from water[236].

Catalysis. Biocarbons have a crucial role in catalysis, offering a sustainable alternative to conventional metallic and oxide catalysts[237]. Biocarbons provide comparable performance, long-term stability, cost effectiveness and tunable surface properties[238]. Biocarbons can be doped with various elements (nitrogen, phosphorus and sulfur) to enhance their performance in processes such as ORR, electrochemical CO_2 reduction[239], hydrogenation[240], pyrolysis of ligno-cellulosic and plastic wastes[241], photo catalysis[242], biofuel production (esterification and transesterification)[243] and water splitting in bio-hydrogen production[70].

Biochar–concrete composites. Biocarbon has also been used in concrete formulations as a sustainable substitute for cement. Biocarbon can enhance concrete properties, serving as a water absorbent, modulus of elasticity enhancer and filler, while contributing to effective carbon sequestration[244]. Biocarbon addition to concrete can improve its workability, setting time, hydration kinetics and durability. Biochar–concrete composites exhibit improved tensile and flexural strength, superior corrosion resistance[245], decreased thermal conductivity and increased sound absorption coefficients[246]. The use of biocarbon in electrified cement holds the potential to transform structures such as houses and roads into energy-storing elements, such as batteries and supercapacitors[247].

Table 2 | Essential information suggested for the development of a comprehensive biocarbon database

Data type	Details required
Composition of biocarbon precursors (raw and pretreated precursors if applicable)	Organic composition
	Macromolecular constituents
	Inorganic content (ash)
	Inorganic composition
Relevant biocarbon production process conditions	Temperature
	Pressure
	Heating rate
	Holding time
	Decomposition atmosphere
	Production method
	Precursors
	Type of reactor
	Post-processing methods
Relevant properties for energy applications	Organic composition
	Inorganic composition
	Surface area
	Pore volume
	Graphitization grade
	Mineral crystalline structure
	Electrical conductivity
Relevant properties for composites	Organic composition
	Inorganic composition
	Surface area
	Pore volume and size distribution
	Surface functional groups
	Hardness and stiffness
	Graphitization grade
Relevant properties for water treatment and gas depollution applications	Organic composition
	Inorganic composition
	Surface functional groups
	Surface area
	Pore volume and size distribution
	pH

Reproducibility and data deposition

The physicochemical properties of biocarbon are highly dependent on the selected precursors, pre-treatments, production methods and process parameters. Moreover, the composition of the raw precursors may be influenced by the growth and harvesting conditions. In accordance with this, similar feedstocks and identical process parameters might be associated with biocarbon materials showing variable properties. As a result, it is still a challenging task to accurately control and reproduce the properties of biocarbon. It is crucial to understand the variability between repeated productions and different feedstocks at laboratory, pilot and industrial scales, which has not been thoroughly addressed[248]. In addition, long-term storage of biocarbon affects its surface functionality, owing to its moisture and gas absorption properties.

The deposition and sharing of data regarding biocarbon properties and process conditions are crucial and may help to overcome reproducibility issues, providing useful information to correlate feedstocks, process conditions and biocarbon properties, helping researchers and industrial actors to better design production protocols adapted to specific biocarbon qualities. The academic community is conducting numerous studies to broaden the horizon of biocarbon application arenas even further. With an increasing number of studies on biocarbon, a data repository could be easily constructed. There are currently no complete databases in this field and it is difficult to compare reproducibility between different research or working groups. The UC Davis Biochar Database is an open source tool led by the University of California that attempts to gather and share biocarbon information. Originally designed for agricultural purposes, the database was extended to include studies related to water and wastewater treatment applications. Machine learning approaches have also been used to gather and compare biocarbon properties from the scientific literature and to look for existing correlations[249]. Creation of extensive databases to correlate biocarbon properties and production methods from different sources is crucial to address reproducibility challenges and establish production protocols and standards. A minimum set of biocarbon characteristics should be provided for effective comparison, as outlined in Table 2. Both the raw feedstock composition and biocarbon production process details are necessary to determine correlations with the resulting biocarbon properties. Deposition and sharing of these data in accessible databases are essential to facilitate comprehensive comparison of biocarbon types.

Limitations and optimizations

Potential supply chain issues

Biocarbon can be derived from various types of biomass, with a preference for waste sources over cultivated sources. Europe annually generates 950 million tons of residual biomass[250]; however, the global distribution of biomass is uneven[251]. Challenges persist in ensuring consistent availability of feedstock with uniform properties. Country-specific biomass can mitigate availability issues, for example, Germany and France have the potential to produce biomass from agricultural residues whereas Sweden and Finland are rich in forestry-waste biomass[252]. Scaling up thermochemical conversion reactors, while retaining the biocarbon properties through process optimization, is essential to the transition to industrial-scale pyrolysis reactors. This demands innovations for efficient biomass feeding, residence time control, heat transfer and energy consumption. Adapting a green chemistry approach for catalytic pyrolysis must be embraced to minimize waste and ensure process efficiency and stability[253].

The plastics industry readily adopts innovative and novel materials, facilitating the market adoption of biocarbon-based polymeric products, with several commercial entities already marketing biocarbon–composite products. As biocarbon can be integrated with polymeric products using the current processing techniques, there is compatibility with the existing production facilities[254]. However, the heterogeneity of biocarbon may lead to product inconsistencies. A major obstacle to the adoption of biocarbon-based products is the lack of internationally recognized standards for materials, environmental and energy applications. Current standards from Europe (European Biochar Certificate) and the USA (International Biochar Initiative) are mostly targeted for agricultural applications. Although efforts are underway to establish national standards in various countries[17], collaboration is crucial to develop a global biocarbon-based circular economy.

Unexpected outcomes and workarounds

Electrical conductivity. The electrical conductivity of biocarbon is a key property with diverse applications. Biocarbon often exists as amorphous or turbostratic structures, resulting in poor conductivity. When they are converted into ordered graphitic carbon, they exhibit in-plane metallic bonding and higher electrical conductivity[255]. Biocarbon materials produced through catalytic pyrolysis at temperatures of 1,000–1,300 °C show superior electrical conductivity; for example, waste jute biomass-derived biocarbon showed electrical conductivity of ~65 S m^{-1}, which is much higher than that of traditional carbon materials (~23 S m^{-1})[256].

Specific surface area. The fundamental physical characteristics of biocarbon, such as specific surface area and pore size distribution, are crucial for applications in environmental remediation and electrochemical energy storage. Studies highlight biocarbon materials with >3,000 $m^2 g^{-1}$ specific surface area achieved through appropriate activation methods. Notably, a biocarbon with a specific surface area of 3,167 $m^2 g^{-1}$ demonstrated excellent CO_2 adsorption performance[257].

Structural and morphological features. A key challenge in biocarbon synthesis is retention of biomass structure during pyrolysis, owing to the polymerization, condensation and carbon stacking mechanisms. Surprisingly, certain types of biomass, such as puffball mushrooms, effectively retain their structure even at high pyrolysis temperatures (750–800 °C), exhibiting excellent performance in electrochemical energy storage[258,259].

Glossary

Biochar
A biocarbon variant produced by pyrolysis of biomass at temperatures ranging from 350 to 900 °C that results in an amorphous or turbostratic structure.

Conducting carbon
Highly conductive carbonaceous materials that are extensively used in batteries and supercapacitors to create electrical channels in electrode material.

Graphitization
The thermal treatment of amorphous or turbostratic carbon above 1,000 °C for prolonged residence times to transform carbon to a more ordered form.

Heteroatom doping
Replacement of carbon atoms in the carbon structure by heteroatoms such as nitrogen, sulfur, phosphorus, oxygen and boron.

Nanoindentation
A method to determine nano- and micro-scale mechanical properties of particulates, thin films, coatings and interfaces by applying a known load on a flat surface and measuring the indented area.

Reinforcement
Fibres or particulates in polymeric composite that effectively participate in stress transfer from polymeric to reinforcement phase.

Outlook

Biocarbon holds potential for applications in materials, environment and energy. Its expanding use spans cutting-edge fields that include electronics, sensors and catalysis, as for conventional carbon materials. Novel applications, such as biocarbon-added concrete to replace high-carbon-footprint cement or substituting for metallurgical coal in steel production, should be explored. The engineered biocompatibility of biocarbon opens avenues for drug delivery. The unique properties of biocarbon can contribute to creating a sustainable-carbon world. Optimal thermochemical conversions of waste-derived biomass and plastics yield biocarbon tailored for high-value material, environmental (including CO_2 capturing and water purification) and energy applications.

Before integrating biocarbon into the bioeconomy, several issues need to be remedied. A robust correlation is required between biomass feedstocks, thermochemical conversion technologies and the resulting biocarbon properties for specific applications. Streamlining the entire process, from biomass collection to thermochemical conversion, in accordance with national and global standards, is essential for consistent biocarbon production. Identifying reliable biomass waste streams is crucial for scalable biocarbon production. Understanding the long-term behaviour, disposal and recyclability of biocarbon in materials and energy applications is necessary. Local and national governments can have a regulatory role in supporting the application potential of biocarbon.

Biocarbon engineering is crucial for tailoring properties to specific applications in biocarbon technology. Balancing biocarbon properties is challenging as certain post-modification processes enhance properties such as electrical conductivity and structural stability, while diminishing others such as number of functional groups. High-temperature-derived graphitic biocarbon promotes physicochemical processes but lacks the functional groups required for applications such as energy storage and environmental remediation. Understanding the relationship between pyrolysis temperature and surface functionality is vital for real-time applications. Biocarbon engineering involves additional processes and multistage protocols,

potentially increasing economic input and manufacturing cost. Using statistical and mathematical tools for experimental design (for example, Taguchi) is recommended for process optimization. Scaling up production, engineering and processing is crucial to meet the growing demand for engineered biocarbon.

Every biomass exhibits unique chemical composition and morphological features, influencing the physicochemical and functional properties of biocarbon. Hence, generalization of the protocols for biomass collection, storage, pre-treatment, pyrolysis and post-modification is challenging. Achieving desired biocarbon properties from diverse biomass feedstocks for specific applications remains challenging. Different combinations may impact the properties of final products, necessitating an understating of feedstock chemical composition. Establishment of a comprehensive biocarbon database is needed to understand the biomass–pyrolysis process–biocarbon property co-relationships. Shifting from localized thermochemical conversion units and/or biomass processing units to a uniform supply–storage–processing system, such as biorefineries, can enhance efficiency and scalability.

Conclusion

Biocarbon is gaining global attention in high-value material applications, transitioning from traditional uses in agriculture and soil amendment. With suitable processes, parameters and post-modifications, nano-structured carbon allotropes such as carbon dots, carbon nanotubes and graphene can be produced. Sustainability and commercial viability of biocarbon technology depend on cost-effective production, application diversity and end-user adaptation. Key approaches, including life-cycle analysis, socio-economic impact studies and techno-economic analysis, are vital for biocarbon-based technologies. Despite its potential in polymeric composites, energy storage and conversion, environmental remediation and sensors, biocarbon faces challenges in feedstock selection, reproducibility, safety, transportation, handling and availability for large-volume applications. These challenges can be addressed through feedstock hybridization, database creation and globally accepted safety protocols. Nevertheless, biocarbon has huge potential to replace traditional carbon materials in various applications, providing advantages for renewability, circularity and sustainability without sacrificing performance.

Published online: 14 March 2024

References

1. Liu, W.-J., Jiang, H. & Yu, H.-Q. Development of biochar-based functional materials: toward a sustainable platform carbon material. *Chem. Rev.* **115**, 12251–12285 (2015).
2. He, M. et al. Waste-derived biochar for water pollution control and sustainable development. *Nat. Rev. Earth Environ.* **3**, 444–460 (2022).
3. Chang, B. P., Rodriguez-Uribe, A., Mohanty, A. K. & Misra, M. A comprehensive review of renewable and sustainable biosourced carbon through pyrolysis in biocomposites uses: current development and future opportunity. *Renew. Sustain. Energy Rev.* **152**, 111666 (2021).
4. Chen, N. & Pilla, S. A comprehensive review on transforming lignocellulosic materials into biocarbon and its utilization for composites applications. *Compos. Part C: Open Access* **7**, 100225 (2022).
5. Weldekidan, H., Mohanty, A. K. & Misra, M. Upcycling of plastic wastes and biomass for sustainable graphitic carbon production: a critical review. *ACS Environ. Au.* **2**, 510–522 (2022).
6. Wang, J. & Wang, S. Preparation, modification and environmental application of biochar: a review. *J. Clean. Prod.* **227**, 1002–1022 (2019).
7. Madhu, R., Periasamy, A. P., Schlee, P., Hérou, S. & Titirici, M.-M. Lignin: a sustainable precursor for nanostructured carbon materials for supercapacitors. *Carbon* **207**, 172–197 (2023).
8. Langhorst, A., Peczonczyk, S., Sun, H., Kiziltas, A. & Mielewski, D. Biocarbon: a lightweight, functional filler for under-the-hood automotive composites. *Polym. Compos.* **43**, 2034–2046 (2022).
9. Cuong, D. V. et al. A critical review on biochar-based engineered hierarchical porous carbon for capacitive charge storage. *Renew. Sustain. Energy Rev.* **145**, 111029 (2021).
10. Pistone, A. & Espro, C. Current trends on turning biomass wastes into carbon materials for electrochemical sensing and rechargeable battery applications. *Curr. Opin. Green Sustain. Chem.* **26**, 100374 (2020).
11. Rawat, S., Wang, C.-T., Lay, C.-H., Hotha, S. & Bhaskar, T. Sustainable biochar for advanced electrochemical/energy storage applications. *J. Energy Storage* **63**, 107115 (2023).
12. Chakraborty, I., Sathe, S., Dubey, B. & Ghangrekar, M. Waste-derived biochar: applications and future perspective in microbial fuel cells. *Bioresour. Technol.* **312**, 123587 (2020).
13. Chai, Y., Wan, C., Cheng, W., Li, X. & Wu, Y. Biomass-derived carbon for dye-sensitized solar cells: a review. *J. Mater. Sci.* **58**, 6057–6075 (2023).
14. Sunyoto, N. M., Zhu, M., Zhang, Z. & Zhang, D. Effect of biochar addition on hydrogen and methane production in two-phase anaerobic digestion of aqueous carbohydrates food waste. *Bioresour. Technol.* **219**, 29–36 (2016).
15. Mohan, D., Sarswat, A., Ok, Y. S. & Pittman, C. U. Jr Organic and inorganic contaminants removal from water with biochar, a renewable, low cost and sustainable adsorbent–a critical review. *Bioresour. Technol.* **160**, 191–202 (2014).
16. Guo, S. et al. Recent advances in biochar-based adsorbents for CO_2 capture. *Carbon Capture Sci. Technol.* **4**, 100059 (2022).
17. Hu, Q. et al. Biochar industry to circular economy. *Sci. Total. Environ.* **757**, 143820 (2021).
18. Foong, S. Y. et al. Valorization of biomass waste to engineered activated biochar by microwave pyrolysis: progress, challenges, and future directions. *Chem. Eng. J.* **389**, 124401 (2020).
19. Xia, L. et al. Climate mitigation potential of sustainable biochar production in China. *Renew. Sustain. Energy Rev.* **175**, 113145 (2023).
20. Matovic, D. Biochar as a viable carbon sequestration option: global and Canadian perspective. *Energy* **36**, 2011–2016 (2011).
21. Tripathi, M., Sahu, J. N. & Ganesan, P. Effect of process parameters on production of biochar from biomass waste through pyrolysis: a review. *Renew. Sustain. Energy Rev.* **55**, 467–481 (2016).
22. Zhang, M., Zhang, J., Ran, S., Sun, W. & Zhu, Z. Biomass-derived sustainable carbon materials in energy conversion and storage applications: status and opportunities. A mini review. *Electrochem. Commun.* **138**, 107283 (2022).
23. Ghodake, G. S. et al. Review on biomass feedstocks, pyrolysis mechanism and physicochemical properties of biochar: state-of-the-art framework to speed up vision of circular bioeconomy. *J. Clean. Prod.* **297**, 126645 (2021).
24. Sun, J., Norouzi, O. & Mašek, O. A state-of-the-art review on algae pyrolysis for bioenergy and biochar production. *Bioresour. Technol.* **346**, 126258 (2022).
25. Gul, E. et al. Production and use of biochar from lignin and lignin-rich residues (such as digestate and olive stones) for wastewater treatment. *J. Anal. Appl. Pyrolysis* **158**, 105263 (2021).
26. Mitchell, P. J., Dalley, T. S. & Helleur, R. J. Preliminary laboratory production and characterization of biochars from lignocellulosic municipal waste. *J. Anal. Appl. Pyrolysis* **99**, 71–78 (2013).
27. Titirici, M. M. et al. Sustainable carbon materials. *Chem. Soc. Rev.* **44**, 250–290 (2015).
28. Parthasarathy, P., Al-Ansari, T., Mackey, H. R., Narayanan, K. S. & McKay, G. A review on prominent animal and municipal wastes as potential feedstocks for solar pyrolysis for biochar production. *Fuel* **316**, 123378 (2022).
29. Yao, M. et al. Recent advances in lignin-based carbon materials and their applications: a review. *Int. J. Biol. Macromol.* **223**, 980–1014 (2022).
30. Li, Y., Gupta, R. & You, S. Machine learning assisted prediction of biochar yield and composition via pyrolysis of biomass. *Bioresour. Technol.* **359**, 127511 (2022).
31. Al-Rumaihi, A., Shahbaz, M., Mckay, G., Mackey, H. & Al-Ansari, T. A review of pyrolysis technologies and feedstock: a blending approach for plastic and biomass towards optimum biochar yield. *Renew. Sustain. Energy Rev.* **167**, 112715 (2022).
32. Wang, T., Zhai, Y., Zhu, Y., Li, C. & Zeng, G. A review of the hydrothermal carbonization of biomass waste for hydrochar formation: process conditions, fundamentals, and physicochemical properties. *Renew. Sustain. Energy Rev.* **90**, 223–247 (2018).
33. Khan, T. A. et al. Hydrothermal carbonization of lignocellulosic biomass for carbon rich material preparation: a review. *Biomass Bioenergy* **130**, 105384 (2019).
34. Titirici, M.-M. & Antonietti, M. Chemistry and materials options of sustainable carbon materials made by hydrothermal carbonization. *Chem. Soc. Rev.* **39**, 103–116 (2010).
35. Zhuang, X. et al. A review on the utilization of industrial biowaste via hydrothermal carbonization. *Renew. Sustain. Energy Rev.* **154**, 111877 (2022).
36. Xiang, W. et al. Biochar technology in wastewater treatment: a critical review. *Chemosphere* **252**, 126539 (2020).
37. Li, Q. et al. Progress in catalytic pyrolysis of municipal solid waste. *Energy Convers. Manage.* **226**, 113525 (2020).
38. Yek, P. N. Y. et al. Progress in the torrefaction technology for upgrading oil palm wastes to energy-dense biochar: a review. *Renew. Sustain. Energy Rev.* **151**, 111645 (2021).
39. Collard, F.-X. & Blin, J. A review on pyrolysis of biomass constituents: mechanisms and composition of the products obtained from the conversion of cellulose, hemicelluloses and lignin. *Renew. Sustain. Energy Rev.* **38**, 594–608 (2014).
40. Patwardhan, P. R., Brown, R. C. & Shanks, B. H. Product distribution from the fast pyrolysis of hemicellulose. *ChemSusChem* **4**, 636–643 (2011).
41. Zhou, S., Pecha, B., van Kuppevelt, M., McDonald, A. G. & Garcia-Perez, M. Slow and fast pyrolysis of Douglas-fir lignin: importance of liquid-intermediate formation on the distribution of products. *Biomass Bioenergy* **66**, 398–409 (2014).

42. McGrath, T. E., Chan, W. G. & Hajaligol, M. R. Low temperature mechanism for the formation of polycyclic aromatic hydrocarbons from the pyrolysis of cellulose. *J. Anal. Appl. Pyrolysis* **66**, 51–70 (2003).
43. Neves, D., Thunman, H., Matos, A., Tarelho, L. & Gómez-Barea, A. Characterization and prediction of biomass pyrolysis products. *Prog. Energy Combust. Sci.* **37**, 611–630 (2011).
44. Wei, L. et al. Characteristics of fast pyrolysis of biomass in a free fall reactor. *Fuel Process. Technol.* **87**, 863–871 (2006).
45. French, R. & Czernik, S. Catalytic pyrolysis of biomass for biofuels production. *Fuel Process. Technol.* **91**, 25–32 (2010).
46. Vassilev, S. V., Baxter, D., Andersen, L. K. & Vassileva, C. G. An overview of the chemical composition of biomass. *Fuel* **89**, 913–933 (2010).
47. Vuppaladadiyam, A. K. et al. A critical review on biomass pyrolysis: reaction mechanisms, process modeling and potential challenges. *J. Energy Inst.* **108**, 101236 (2023).
48. Li, L., Long, A., Fossum, B. & Kaiser, M. Effects of pyrolysis temperature and feedstock type on biochar characteristics pertinent to soil carbon and soil health: a meta-analysis. *Soil. Use Manage.* **39**, 43–52 (2023).
49. Zhao, B. et al. Effect of pyrolysis temperature, heating rate, and residence time on rapeseed stem derived biochar. *J. Clean. Prod.* **174**, 977–987 (2018).
50. Kong, X. et al. Synthesis of graphene-like carbon from biomass pyrolysis and its applications. *Chem. Eng. J.* **399**, 125808 (2020).
51. Ghogia, A. C., Romero Millán, L. M., White, C. E. & Nzihou, A. Synthesis and growth of green graphene from biochar revealed by magnetic properties of iron catalyst. *ChemSusChem* **16**, e202201864 (2023).
52. Dai, L. et al. Tuning oxygenated functional groups on biochar for water pollution control: a critical review. *J. Hazard. Mater.* **420**, 126547 (2021).
53. Weber, K. & Quicker, P. Properties of biochar. *Fuel* **217**, 240–261 (2018).
54. Cheng, B.-H., Zeng, R. J. & Jiang, H. Recent developments of post-modification of biochar for electrochemical energy storage. *Bioresour. Technol.* **246**, 224–233 (2017).
55. Foo, K. & Hameed, B. Coconut husk derived activated carbon via microwave induced activation: effects of activation agents, preparation parameters and adsorption performance. *Chem. Eng. J.* **184**, 57–65 (2012).
56. Gupta, R. K., Dubey, M., Kharel, P., Gu, Z. & Fan, Q. H. Biochar activated by oxygen plasma for supercapacitors. *J. Power Sources* **274**, 1300–1305 (2015).
57. Adhamash, E., Pathak, R., Qiao, Q., Zhou, Y. & McTaggart, R. Gamma-radiated biochar carbon for improved supercapacitor performance. *RSC Adv.* **10**, 29910–29917 (2020).
58. Sangtong, N. et al. Ultrahigh-surface-area activated biocarbon based on biomass residue as a supercapacitor electrode material: tuning pore structure using alkalis with different atom sizes. *Microporous Mesoporous Mater.* **326**, 111383 (2021).
59. Purkait, T., Singh, G., Singh, M., Kumar, D. & Dey, R. S. Large area few-layer graphene with scalable preparation from waste biomass for high-performance supercapacitor. *Sci. Rep.* **7**, 15239 (2017).
60. Goswami, S., Banerjee, P., Datta, S., Mukhopadhayay, A. & Das, P. Graphene oxide nanoplatelets synthesized with carbonized agro-waste biomass as green precursor and its application for the treatment of dye rich wastewater. *Process. Saf. Environ. Prot.* **106**, 163–172 (2017).
61. Saliu, O., Adeniyi, A., Mamo, M., Ndungu, P. & Ramontja, J. Microwave exfoliation of a biochar obtained from updraft retort carbonization for supercapacitor fabrication. *Electrochem. Commun.* **139**, 107308 (2022).
62. Yan, Y., Manickam, S., Lester, E., Wu, T. & Pang, C. H. Synthesis of graphene oxide and graphene quantum dots from miscanthus via ultrasound-assisted mechano-chemical cracking method. *Ultrason. Sonochem.* **73**, 105519 (2021).
63. Bukhari, Q. U. A. et al. Water-phase exfoliated biochar nanofibers from eucalyptus scraps for electrode modification and conductive film fabrication. *ACS Sustain. Chem. Eng.* **9**, 13988–13998 (2021).
64. Farid, M. A. A. & Andou, Y. A route towards graphene from lignocellulosic biomass: technicality, challenges, and their prospective applications. *J. Clean. Prod.* **388**, 135090 (2022).
65. Genovese, M., Jiang, J., Lian, K. & Holm, N. High capacitive performance of exfoliated biochar nanosheets from biomass waste corn cob. *J. Mater. Chem. A* **3**, 2903–2913 (2015).
66. Chatterjee, R. et al. Ultrasound cavitation intensified amine functionalization: a feasible strategy for enhancing CO_2 capture capacity of biochar. *Fuel* **225**, 287–298 (2018).
67. Qi, X. et al. A simple and recyclable molten-salt route to prepare superthin biocarbon sheets based on the high water-absorbent agaric for efficient lithium storage. *Carbon* **157**, 286–294 (2020).
68. Lu, J., Drzal, L. T., Worden, R. M. & Lee, I. Simple fabrication of a highly sensitive glucose biosensor using enzymes immobilized in exfoliated graphite nanoplatelets nafion membrane. *Chem. Mater.* **19**, 6240–6246 (2007).
69. Escobar, B., Pérez-Salcedo, K., Alonso-Lemus, I., Pacheco, D. & Barbosa, R. *N*-doped porous carbon from *Sargassum* spp. as metal-free electrocatalysts for oxygen reduction reaction in alkaline media. *Int. J. Hydrog. Energy* **42**, 30274–30283 (2017).
70. Xia, C. et al. A sulfur self-doped multifunctional biochar catalyst for overall water splitting and a supercapacitor from *Camellia japonica* flowers. *Carbon Energy* **4**, 491–505 (2022).
71. Reimer, C. et al. Synthesis and characterization of novel nitrogen doped biocarbons from distillers dried grains with solubles (DDGS) for supercapacitor applications. *Bioresour. Technol. Rep.* **9**, 100375 (2020).
72. Marrakchi, F., Zafar, F. F., Wei, M., Cao, B. & Wang, S. N-doped mesoporous H_3PO_4–pyrocarbon from seaweed and melamine for batch adsorption of the endocrine disruptor bisphenol A. *J. Mol. Liq.* **345**, 117040 (2022).
73. Anstey, A., Vivekanandhan, S., Rodriguez-Uribe, A., Misra, M. & Mohanty, A. K. Oxidative acid treatment and characterization of new biocarbon from sustainable *Miscanthus* biomass. *Sci. Total. Environ.* **550**, 241–247 (2016).
74. Wang, Y. et al. Steam reforming of acetic acid over Ni/biochar catalyst treated with HNO3: impacts of the treatment on surface properties and catalytic behaviors. *Fuel* **278**, 118341 (2020).
75. Chen, H., Han, X. & Liu, Y. Gaseous hydrogen sulfide removal using macroalgae biochars modified synergistically by H_2SO_4/H_2O_2. *Chem. Eng. Technol.* **44**, 698–709 (2021).
76. Sizmur, T., Fresno, T., Akgül, G., Frost, H. & Moreno-Jiménez, E. Biochar modification to enhance sorption of inorganics from water. *Bioresour. Technol.* **246**, 34–47 (2017).
77. Das, O., Sarmah, A. K. & Bhattacharyya, D. Structure–mechanics property relationship of waste derived biochars. *Sci. Total. Environ.* **538**, 611–620 (2015).
78. Chen, H. et al. KOH modification effectively enhances the Cd and Pb adsorption performance of N-enriched biochar derived from waste chicken feathers. *Waste Manage.* **130**, 82–92 (2021).
79. Dewage, N. B., Fowler, R. E., Pittman, C. U., Mohan, D. & Mlsna, T. Lead (Pb^{2+}) sorptive removal using chitosan-modified biochar: batch and fixed-bed studies. *RSC Adv.* **8**, 25368–25377 (2018).
80. Xu, Y. et al. Enhanced adsorption of methylene blue by citric acid modification of biochar derived from water hyacinth (Eichornia crassipes). *Environ. Sci. Pollut. Res.* **23**, 23606–23618 (2016).
81. Saremi, F., Miroliaei, M. R., Nejad, M. S. & Sheibani, H. Adsorption of tetracycline antibiotic from aqueous solutions onto vitamin B6-upgraded biochar derived from date palm leaves. *J. Mol. Liq.* **318**, 114126 (2020).
82. Tomczyk, A. & Szewczuk-Karpisz, K. Effect of biochar modification by vitamin c, hydrogen peroxide or silver nanoparticles on its physicochemistry and tetracycline removal. *Materials* **15**, 5379 (2022).
83. Hosny, M., Fawzy, M. & Eltaweil, A. S. Phytofabrication of bimetallic silver-copper/biochar nanocomposite for environmental and medical applications. *J. Environ. Manage.* **316**, 115238 (2022).
84. Tong, J. et al. Composite of FeCo alloy embedded in biocarbon derived from eggshell membrane with high performance for oxygen reduction reaction and supercapacitor. *Electrochim. Acta* **248**, 388–396 (2017).
85. Qian, C. et al. Co_3O_4 nanoparticles on porous bio-carbon substrate as catalyst for oxygen reduction reaction. *Microporous Mesoporous Mater.* **277**, 45–51 (2019).
86. Mahajan, H., Mohanan, K. U. & Cho, S. Facile synthesis of biocarbon-based MoS_2 composite for high-performance supercapacitor application. *Nano Lett.* **22**, 8161–8167 (2022).
87. Zhang, D. et al. High-performance battery-type supercapacitor based on porous biocarbon and biocarbon supported Ni–Co layered double hydroxide. *J. Alloys Compd.* **837**, 155529 (2020).
88. Yang, X., Jiang, Z., Fei, B., Ma, J. & Liu, X. Graphene functionalized bio-carbon xerogel for achieving high-rate and high-stability supercapacitors. *Electrochim. Acta* **282**, 813–821 (2018).
89. Liang, C. et al. Ultra-light MXene aerogel/wood-derived porous carbon composites with wall-like "mortar/brick" structures for electromagnetic interference shielding. *Sci. Bull.* **65**, 616–622 (2020).
90. Yang, B.-J., Jiang, L.-L., Li, Y.-J., Cai, F.-G. & Zhang, Q.-Y. Three-dimensional porous biocarbon wrapped by graphene and polypyrrole composite as electrode materials for supercapacitor. *J. Mater. Sci. Mater. Electron.* **29**, 2568–2572 (2018).
91. Kaushal, I., Saharan, P., Kumar, V., Sharma, A. K. & Umar, A. Superb sono-adsorption and energy storage potential of multifunctional Ag-Biochar composite. *J. Alloys Compd.* **785**, 240–249 (2019).
92. Zhang, Y. et al. Synthesis of γ-Fe_2O_3-ZnO-biochar nanocomposites for rhodamine B removal. *Appl. Surf. Sci. Adv.* **501**, 144217 (2020).
93. Endler, L. W., Wolfart, F., Mangrich, A. S., Vidotti, M. & Marchesi, L. F. Facile method to prepare biochar–NiO nanocomposites as a promisor material for electrochemical energy storage devices. *Chem. Pap.* **74**, 1471–1476 (2020).
94. Chen, T. et al. Three dimensional hierarchical porous nickel cobalt layered double hydroxides (LDHs) and nitrogen doped activated biocarbon composites for high-performance asymmetric supercapacitor. *J. Alloys Compd.* **859**, 158318 (2021).
95. Mao, W., Zhang, Y., Luo, J., Chen, L. & Guan, Y. Novel co-polymerization of polypyrrole/polyaniline on ferrate modified biochar composites for the efficient adsorption of hexavalent chromium in water. *Chemosphere* **303**, 135254 (2022).
96. Thomas, D., Fernandez, N. B., Mullassery, M. D. & Surya, R. Iron oxide loaded biochar/polyaniline nanocomposite: synthesis, characterization and electrochemical analysis. *Inorg. Chem. Commun.* **119**, 108097 (2020).
97. Thines, K., Abdullah, E., Mubarak, N. & Ruthiraan, M. In-situ polymerization of magnetic biochar–polypyrrole composite: a novel application in supercapacitor. *Biomass Bioenergy* **98**, 95–111 (2017).
98. Sigmund, G. et al. Cytotoxicity of biochar: a workplace safety concern? *Environ. Sci. Technol. Lett.* **4**, 362–366 (2017).
99. Zhang, J. et al. Chronic carbon black nanoparticles exposure increases lung cancer risk by affecting the cell cycle via circulatory inflammation. *Environ. Pollut.* **305**, 119293 (2022).
100. Ogle, R. A. in *Dust Explosion Dynamics* ch. 1 (Elsevier, 2017).
101. Center for Chemical Process Safety. *Guidelines for Combustible Dust Hazard Analysis* (Wiley, 2017).
102. Zhao, M. Y., Enders, A. & Lehmann, J. Short-and long-term flammability of biochars. *Biomass Bioenergy* **69**, 183–191 (2014).

103. Restuccia, F., Mašek, O., Hadden, R. M. & Rein, G. Quantifying self-heating ignition of biochar as a function of feedstock and the pyrolysis reactor temperature. *Fuel* **236**, 201–213 (2019).
104. del Campo, B., Brumm, T. & Keren, N. Fast pyrolysis biochar flammability behavior for handling and storage. *ACI Av. en. Cienc. e Ingenierías* **13**, 23 (2021).
105. Enders, A. & Lehmann, J. in *Biochar: A Guide to Analytical Methods* (eds Singh, B., Camps-Arbestain, M. & Lehmann, J.) 9–22 (2017).
106. Igalavithana, A. D. et al. Advances and future directions of biochar characterization methods and applications. *Crit. Rev. Env. Sci. Technol.* **47**, 2275–2330 (2017).
107. Li, S. & Chen, G. Thermogravimetric, thermochemical, and infrared spectral characterization of feedstocks and biochar derived at different pyrolysis temperatures. *Waste Manage.* **78**, 198–207 (2018).
108. Singh, B., Fang, Y., Cowie, B. C. & Thomsen, L. NEXAFS and XPS characterisation of carbon functional groups of fresh and aged biochars. *Org. Geochem.* **77**, 1–10 (2014).
109. Nanda, S. et al. Characterization of North American lignocellulosic biomass and biochars in terms of their candidacy for alternate renewable fuels. *Bioenergy Res.* **6**, 663–677 (2013).
110. Blanco-Canqui, H. Biochar and soil physical properties. *Soil Sci. Soc. Am. J.* **81**, 687–711 (2017).
111. Kang, S., Jung, J., Choe, J. K., Ok, Y. S. & Choi, Y. Effect of biochar particle size on hydrophobic organic compound sorption kinetics: applicability of using representative size. *Sci. Total. Environ.* **619**, 410–418 (2018).
112. Khiari, Z., Alka, K., Kelloway, S., Mason, B. & Savidov, N. Integration of biochar filtration into aquaponics: effects on particle size distribution and turbidity removal. *Agric. Water Manage.* **229**, 105874 (2020).
113. Liao, W. & Thomas, S. C. Biochar particle size and post-pyrolysis mechanical processing affect soil pH, water retention capacity, and plant performance. *Soil Syst.* **3**, 14 (2019).
114. Ma, X. et al. Study of biochar properties by scanning electron microscope–energy dispersive X-ray spectroscopy (SEM-EDX). *Commun. Soil Sci. Plant Anal.* **47**, 593–601 (2016).
115. Elkhalifa, S. et al. Biochar development from thermal TGA studies of individual food waste vegetables and their blended systems. *Biomass Convers. Biorefin.* https://doi.org/10.1007/s13399-022-02441-0 (2022).
116. O'reilly, J. & Mosher, R. Functional groups in carbon black by FTIR spectroscopy. *Carbon* **21**, 47–51 (1983).
117. Xu, J. et al. Raman spectroscopy of biochar from the pyrolysis of three typical Chinese biomasses: a novel method for rapidly evaluating the biochar property. *Energy* **202**, 117644 (2020).
118. McBeath, A. V., Smernik, R. J., Krull, E. S. & Lehmann, J. The influence of feedstock and production temperature on biochar carbon chemistry: a solid-state 13C NMR study. *Biomass Bioenergy* **60**, 121–129 (2014).
119. Mousavi-Avval, S. H., Sahoo, K., Nepal, P., Runge, T. & Bergman, R. Environmental impacts and techno-economic assessments of biobased products: a review. *Renew. Sustain. Energy Rev.* **180**, 113302 (2023).
120. Sahoo, K. et al. Life-cycle assessment and techno-economic analysis of biochar produced from forest residues using portable systems. *Int. J. Life Cycle Assess.* **26**, 189–213 (2021).
121. Mishra, R. K., Kumar, D. J. P., Narula, A., Chistie, S. M. & Naik, S. U. Production and beneficial impact of biochar for environmental application: a review on types of feedstocks, chemical compositions, operating parameters, techno-economic study, and life cycle assessment. *Fuel* **343**, 127968 (2023).
122. Haeldermans, T. et al. A comparative techno-economic assessment of biochar production from different residue streams using conventional and microwave pyrolysis. *Bioresour. Technol.* **318**, 124083 (2020).
123. Fawzy, S. et al. Atmospheric carbon removal via industrial biochar systems: a techno-economic-environmental study. *J. Clean. Prod.* **371**, 133660 (2022).
124. Nematian, M., Keske, C. & Ng'ombe, J. N. A techno-economic analysis of biochar production and the bioeconomy for orchard biomass. *Waste Manage.* **135**, 467–477 (2021).
125. Alhashimi, H. A. & Aktas, C. B. Life cycle environmental and economic performance of biochar compared with activated carbon: a meta-analysis. *Resour. Conserv. Recycl.* **118**, 13–26 (2017).
126. Campbell, R. M., Anderson, N. M., Daugaard, D. E. & Naughton, H. T. Financial viability of biofuel and biochar production from forest biomass in the face of market price volatility and uncertainty. *Appl. Energy* **230**, 330–343 (2018).
127. Shabangu, S., Woolf, D., Fisher, E. M., Angenent, L. T. & Lehmann, J. Techno-economic assessment of biomass slow pyrolysis into different biochar and methanol concepts. *Fuel* **117**, 742–748 (2014).
128. Lehmann, J. A handful of carbon. *Nature* **447**, 143–144 (2007).
129. Ibarrola, R., Shackley, S. & Hammond, J. Pyrolysis biochar systems for recovering biodegradable materials: a life cycle carbon assessment. *Waste Manage.* **32**, 859–868 (2012).
130. Roberts, K. G., Gloy, B. A., Joseph, S., Scott, N. R. & Lehmann, J. Life cycle assessment of biochar systems: estimating the energetic, economic, and climate change potential. *Environ. Sci. Technol.* **44**, 827–833 (2010).
131. Hammond, J., Shackley, S., Sohi, S. & Brownsort, P. Prospective life cycle carbon abatement for pyrolysis biochar systems in the UK. *Energy Policy* **39**, 2646–2655 (2011).
132. Muñoz, E., Curaqueo, G., Cea, M., Vera, L. & Navia, R. Environmental hotspots in the life cycle of a biochar-soil system. *J. Clean. Prod.* **158**, 1–7 (2017).
133. George, J., Jung, D. & Bhattacharyya, D. Improvement of electrical and mechanical properties of PLA/PBAT composites using coconut shell biochar for antistatic applications. *Appl. Sci.* **13**, 902 (2023).
134. Poulose, A. M. et al. Date palm biochar-polymer composites: an investigation of electrical, mechanical, thermal and rheological characteristics. *Sci. Total Environ.* **619**, 311–318 (2018).
135. Sobhan, A. et al. Development and characterization of a novel activated biochar-based polymer composite for biosensors. *Int. J. Polym. Anal. Charact.* **26**, 544–560 (2021).
136. Das, O., Sarmah, A. K. & Bhattacharyya, D. Nanoindentation assisted analysis of biochar added biocomposites. *Compos. Part B* **91**, 219–227 (2016).
137. Jurkiewicz, K. et al. Evolution of glassy carbon under heat treatment: correlation structure–mechanical properties. *J. Mater. Sci.* **53**, 3509–3523 (2018).
138. Zickler, G., Schöberl, T. & Paris, O. Mechanical properties of pyrolysed wood: a nanoindentation study. *Philos. Mag.* **86**, 1373–1386 (2006).
139. Das, O. et al. Flammability and mechanical properties of biochars made in different pyrolysis reactors. *Biomass Bioenergy* **152**, 106197 (2021).
140. Shanmugam, V. et al. A review on combustion and mechanical behaviour of pyrolysis biochar. *Mater. Today Commun.* **31**, 103629 (2022).
141. Das, O., Sarmah, A. K. & Bhattacharyya, D. Biocomposites from waste derived biochars: mechanical, thermal, chemical, and morphological properties. *Waste Manage.* **49**, 560–570 (2016).
142. Minugu, O. P., Gujjala, R., Shakuntala, O., Manoj, P. & Chowdary, M. S. Effect of biomass derived biochar materials on mechanical properties of biochar epoxy composites. *Proc. Inst. Mech. Eng. Part. C: J. Mech.* **235**, 5626–5638 (2021).
143. Jiang, C. et al. Converting waste lignin into nano-biochar as a renewable substitute of carbon black for reinforcing styrene-butadiene rubber. *Waste Manage.* **102**, 732–742 (2020).
144. Tan, X. F. et al. Role of biochar surface characteristics in the adsorption of aromatic compounds: pore structure and functional groups. *Chin. Chem. Lett.* **32**, 2939–2946 (2021).
145. Zhang, Q. et al. Properties evaluation of biochar/high-density polyethylene composites: emphasizing the porous structure of biochar by activation. *Sci. Total. Environ.* **737**, 139770 (2020).
146. Zainal Abidin, Z., Mamauod, S. N. L., Romli, A. Z., Sarkawi, S. S. & Zainal, N. H. Synergistic effect of partial replacement of carbon black by palm kernel shell biochar in carboxylated nitrile butadiene rubber composites. *Polymers* **15**, 943 (2023).
147. Janu, R. et al. Biochar surface functional groups as affected by biomass feedstock, biochar composition and pyrolysis temperature. *Carbon Resour. Convers.* **4**, 36–46 (2021).
148. Das, O., Kim, N. K., Sarmah, A. K. & Bhattacharyya, D. Development of waste based biochar/wool hybrid biocomposites: flammability characteristics and mechanical properties. *J. Clean. Prod.* **144**, 79–89 (2017).
149. Liu, Z., Fei, B. & Jiang, Z. Combustion characteristics of bamboo-biochars. *Bioresour. Technol.* **167**, 94–99 (2014).
150. Codou, A., Misra, M. & Mohanty, A. K. Sustainable biocarbon reinforced nylon 6/polypropylene compatibilized blends: effect of particle size and morphology on performance of the biocomposites. *Compos. Part A* **112**, 1–10 (2018).
151. Nagarajan, V., Mohanty, A. K. & Misra, M. Biocomposites with size-fractionated biocarbon: influence of the microstructure on macroscopic properties. *ACS Omega* **1**, 636–647 (2016).
152. Ogunsona, E. O., Misra, M. & Mohanty, A. K. Sustainable biocomposites from biobased polyamide 6, 10 and biocarbon from pyrolyzed miscanthus fibers. *J. Appl. Polym. Sci.* **134**, 44221 (2017).
153. Ikram, S., Das, O. & Bhattacharyya, D. A parametric study of mechanical and flammability properties of biochar reinforced polypropylene composites. *Compos. Part A* **91**, 177–188 (2016).
154. Jayabalakrishnan, D. et al. Mechanical, dielectric, and hydrophobicity behavior of coconut shell biochar toughened Caryota urens natural fiber reinforced epoxy composite. *Polym. Compos.* **43**, 493–502 (2021).
155. Peterson, S. C. & Kim, S. Reducing biochar particle size with nanosilica and its effect on rubber composite reinforcement. *J. Polym. Environ.* **28**, 317–322 (2020).
156. DeVallance, D. B., Oporto, G. S. & Quigley, P. Investigation of hardwood biochar as a replacement for wood flour in wood–polypropylene composites. *J. Elastomers Plast.* **48**, 510–522 (2016).
157. Chang, B. P. et al. Effect of a small amount of synthetic fiber on performance of biocarbon-filled nylon-based hybrid biocomposites. *Macromol. Mater. Eng.* **306**, 2000680 (2021).
158. Alshahrani, H. & Prakash, V. A. Effect of silane-grafted orange peel biochar and areca fibre on mechanical, thermal conductivity and dielectric properties of epoxy resin composites. *Biomass Convers. Biorefin.* https://doi.org/10.1007/s13399-022-02801-w (2022).
159. Greenough, S., Dumont, M.-J. & Prasher, S. The physicochemical properties of biochar and its applicability as a filler in rubber composites: a review. *Mater. Today Commun.* **29**, 102912 (2021).
160. Peterson, S. C. Utilization of low-ash biochar to partially replace carbon black in styrene–butadiene rubber composites. *J. Elastomers Plast.* **45**, 487–497 (2013).
161. Peterson, S. C., Chandrasekaran, S. R. & Sharma, B. K. Birchwood biochar as partial carbon black replacement in styrene–butadiene rubber composites. *J. Elastomers Plast.* **48**, 305–316 (2016).

162. Alhelal, A., Mohammed, Z., Jeelani, S. & Rangari, V. K. 3D printing of spent coffee ground derived biochar reinforced epoxy composites. *J. Compos. Mater.* **55**, 3651–3660 (2021).
163. Idrees, M., Jeelani, S. & Rangari, V. Three-dimensional-printed sustainable biochar-recycled PET composites. *ACS Sustain. Chem. Eng.* **6**, 13940–13948 (2018).
164. Mohammed, Z., Jeelani, S. & Rangari, V. Effective reinforcement of engineered sustainable biochar carbon for 3D printed polypropylene biocomposites. *Compos. Part C: Open Access* **7**, 100221 (2022).
165. Behazin, E., Misra, M. & Mohanty, A. K. Compatibilization of toughened polypropylene/biocarbon biocomposites: a full factorial design optimization of mechanical properties. *Polym. Test.* **61**, 364–372 (2017).
166. Behazin, E., Misra, M. & Mohanty, A. K. Sustainable biocomposites from pyrolyzed grass and toughened polypropylene: structure–property relationships. *ACS Omega* **2**, 2191–2199 (2017).
167. Tadele, D. *Environmental Life Cycle Assessment of Biomaterials and Bio-Composites for Automotive Components: A Comparison between Talc and Biochar Reinforced Polypropylene Composites*. Thesis, Univ. Guelph (2019).
168. Tadele, D., Roy, P., Defersha, F., Misra, M. & Mohanty, A. K. A comparative life-cycle assessment of talc-and biochar-reinforced composites for lightweight automotive parts. *Clean Technol. Environ. Policy* **22**, 639–649 (2020).
169. Wallace, C. A., Saha, G. C., Afzal, M. T. & Lloyd, A. Experimental and computational modeling of effective flexural/tensile properties of microwave pyrolysis biochar reinforced GFRP biocomposites. *Compos. Part B* **175**, 107180 (2019).
170. Huang, Y. et al. Multifunctional energy storage and conversion devices. *Adv. Mater.* **28**, 8344–8364 (2016).
171. Rahman, M. Z., Edvinsson, T. & Kwong, P. Biochar for electrochemical applications. *Curr. Opin. Green Sustain. Chem.* **23**, 25–30 (2020).
172. Liu, W.-J., Jiang, H. & Yu, H.-Q. Emerging applications of biochar-based materials for energy storage and conversion. *Energy Environ. Sci.* **12**, 1751–1779 (2019).
173. Yue, M. et al. Hydrogen energy systems: a critical review of technologies, applications, trends and challenges. *Renew. Sustain. Energy Rev.* **146**, 111180 (2021).
174. Niaz, S., Manzoor, T. & Pandith, A. H. Hydrogen storage: materials, methods and perspectives. *Renew. Sustain. Energy Rev.* **50**, 457–469 (2015).
175. Chouikhi, N. et al. Valorization of agricultural waste as a carbon materials for selective separation and storage of CO_2, H_2 and N_2. *Biomass Bioenergy* **155**, 106297 (2021).
176. Pedicini, R. et al. Posidonia oceanica and wood chips activated carbon as interesting materials for hydrogen storage. *Int. J. Hydrog. Energy* **45**, 14038–14047 (2020).
177. Liang, Y. et al. Preparation and hydrogen storage performance of poplar sawdust biochar with high specific surface area. *Ind. Crop. Prod.* **200**, 116788 (2023).
178. Klasson, K. T., Uchimiya, M. & Lima, I. M. Characterization of narrow micropores in almond shell biochars by nitrogen, carbon dioxide, and hydrogen adsorption. *Ind. Crop. Prod.* **67**, 33–40 (2015).
179. Stock, S. et al. Coffee waste-derived nanoporous carbons for hydrogen storage. *ACS Appl. Energy Mater.* **5**, 10915–10926 (2022).
180. Harry, K. J., Hallinan, D. T., Parkinson, D. Y., MacDowell, A. A. & Balsara, N. P. Detection of subsurface structures underneath dendrites formed on cycled lithium metal electrodes. *Nat. Mater.* **13**, 69–73 (2014).
181. Wu, Y., Rahm, E. & Holze, R. Carbon anode materials for lithium ion batteries. *J. Power Sources* **114**, 228–236 (2003).
182. Mullaivananathan, V., Sathish, R. & Kalaiselvi, N. Coir pith derived bio-carbon: demonstration of potential anode behavior in lithium-ion batteries. *Electrochim. Acta* **225**, 143–150 (2017).
183. Nagalakshmi, M. & Kalaiselvi, N. Mesoporous dominant cashewnut sheath derived bio-carbon anode for LIBs and SIBs. *Electrochim. Acta* **304**, 175–183 (2019).
184. Wang, Y., Chang, H., Ma, T., Deng, H. & Zha, Z. Effect of cotton stalk particle size on the structure of biochar and the performance of anode for lithium-ion battery. *J. Phys. Chem. Solids* **169**, 110845 (2022).
185. Xie, F., Xu, Z., Guo, Z. & Titirici, M.-M. Hard carbons for sodium-ion batteries and beyond. *Prog. Energy* **2**, 042002 (2020).
186. Senthil, C. & Lee, C. W. Biomass-derived biochar materials as sustainable energy sources for electrochemical energy storage devices. *Renew. Sustain. Energy Rev.* **137**, 110464 (2021).
187. Rahman, M. A., Wang, X. & Wen, C. High energy density metal-air batteries: a review. *J. Electrochem. Soc.* **160**, A1759 (2013).
188. Qiao, Y. et al. Activated biochar derived from peanut shells as the electrode materials with excellent performance in zinc-air battery and supercapacitance. *Waste Manage.* **125**, 257–267 (2021).
189. Miao, W. et al. Cobalt (iron), nitrogen and carbon doped mushroom biochar for high-efficiency oxygen reduction in microbial fuel cell and Zn-air battery. *J. Environ. Chem. Eng.* **10**, 108474 (2022).
190. Han, S. et al. In situ exfoliated graphene-like carbon nanosheets strongly coupled with the biochar tube as the cathode for an application-ready Zn-air battery. *ACS Appl. Energy Mater.* **5**, 14423–14432 (2022).
191. Han, S. et al. Boosting the electrochemical performance of Zn-air battery with N/O co-doped biochar catalyst via a simple physical strategy of forced convection intensity. *Chem. Eng. Sci.* **272**, 118615 (2023).
192. Cao, R., Lee, J. S., Liu, M. & Cho, J. Recent progress in non-precious catalysts for metal-air batteries. *Adv. Energy Mater.* **2**, 816–829 (2012).
193. Lei, X. et al. Nitrogen-doped micropore-dominant carbon derived from waste pine cone as a promising metal-free electrocatalyst for aqueous zinc/air batteries. *J. Power Sources* **365**, 76–82 (2017).
194. Sumangala Devi, N., Hariram, M. & Vivekanandhan, S. Modification techniques to improve the capacitive performance of biocarbon materials. *J. Energy Storage* **33**, 101870 (2021).
195. Yumak, T. et al. Comparison of the electrochemical properties of engineered switchgrass biomass-derived activated carbon-based EDLCs. *Colloids Surf. A* **586**, 124150 (2020).
196. Zhang, W. et al. Lignin derived porous carbons: synthesis methods and supercapacitor applications. *Small Methods* **5**, 2100896 (2021).
197. Zhu, H., Wang, X., Yang, F. & Yang, X. Promising carbons for supercapacitors derived from fungi. *Adv. Mater.* **23**, 2745–2748 (2011).
198. Hou, Z. Q. et al. Algae-based carbons: design, preparation and recent advances in their use in energy storage, catalysis and adsorption. *N. Carbon Mater.* **36**, 278–303 (2021).
199. Naik, P. B. et al. Developing high-performance flexible zinc ion capacitors from agricultural waste-derived carbon sheets. *ACS Sustain. Chem. Eng.* **10**, 1471–1481 (2022).
200. Sennu, P., Arun, N., Madhavi, S., Aravindan, V. & Lee, Y.-S. All carbon based high energy lithium-ion capacitors from biomass: the role of crystallinity. *J. Power Sources* **414**, 96–102 (2019).
201. Payá, S., Díez, N. & Sevilla, M. Biomass-derived carbon sponges for use as sodium-ion capacitor electrodes. *Sustain. Energy Fuels* **7**, 2378–2389 (2023).
202. Codou, A., Pin, J.-M., Misra, M. & Mohanty, A. K. Impact of temperature and in situ FeCo catalysis on the architecture and Young's modulus of model wood-based biocarbon. *Green Chem.* **23**, 3015–3027 (2021).
203. Kane, S., Storer, A., Xu, W., Ryan, C. & Stadie, N. P. Biochar as a renewable substitute for carbon black in lithium-ion battery electrodes. *ACS Sustain. Chem. Eng.* **10**, 12226–12233 (2022).
204. Weldekidan, H., Vivekanandhan, S., Tripathi, N., Mohanty, A. K. & Misra, M. Highly conductive biocarbon nanostructures from burlap waste as a sustainable additive for supercapacitor electrodes. *Mater. Adv.* **5**, 1240–1250 (2024).
205. Steele, B. C. & Heinzel, A. Materials for fuel-cell technologies. *Nature* **414**, 345–352 (2001).
206. Shen, Y. et al. Lignin derived multi-doped (N, S, Cl) carbon materials as excellent electrocatalyst for oxygen reduction reaction in proton exchange membrane fuel cells. *J. Energy Chem.* **44**, 106–114 (2020).
207. Im, K., Choi, K. H., Park, B. J., Yoo, S. J. & Kim, J. Tofu-derived heteroatom-doped carbon for oxygen reduction reaction in an anion exchange membrane–fuel cell. *Energy Convers. Manage.* **265**, 115754 (2022).
208. Huang, T., Wei, J., Zhu, X. & Zhang, E. Soybean powder enables the synthesis of Fe–N–C catalysts with high ORR activities in microbial fuel cell applications. *Int. J. Hydrog. Energy* **46**, 30334–30343 (2021).
209. Noorasid, N. S. et al. Current advancement of flexible dye sensitized solar cell: a review. *Optik* **254**, 168089 (2022).
210. Briscoe, J., Marinovic, A., Sevilla, M., Dunn, S. & Titirici, M. Biomass-derived carbon quantum dot sensitizers for solid-state nanostructured solar cells. *Angew. Chem. Int. Ed.* **54**, 4463–4468 (2015).
211. Rezaei, B., Irannejad, N., Ensafi, A. A. & Kazemifard, N. The impressive effect of eco-friendly carbon dots on improving the performance of dye-sensitized solar cells. *Sol. Energy* **182**, 412–419 (2019).
212. Yoon, C. H., Chul, S. K., Ko, H. H., Yi, S. & Jeong, S. H. Enhanced performance of dye-sensitized solar cells with activated carbons. *J. Nanosci. Nanotechnol.* **13**, 7875–7879 (2013).
213. Vivekanandhan, S. Recent developments and emerging opportunities for biomass derived carbon materials in dye sensitized solar energy conversion. *ChemBioEngRev* **10**, 993–1005 (2023).
214. Zhang, J., Yang, M., Zhao, W., Zhang, J. & Zang, L. Biohydrogen production amended with nitrogen-doped biochar. *Energy Fuels* **35**, 1476–1487 (2021).
215. Bhatia, S. K. et al. Trends in renewable energy production employing biomass-based biochar. *Bioresour. Technol.* **340**, 125644 (2021).
216. Bu, J., Wei, H.-L., Wang, Y.-T., Cheng, J.-R. & Zhu, M.-J. Biochar boosts dark fermentative H_2 production from sugarcane bagasse by selective enrichment/colonization of functional bacteria and enhancing extracellular electron transfer. *Water Res.* **202**, 117440 (2021).
217. Wu, J.-w, Pei, S.-z, Zhou, C.-s, Liu, B.-f & Cao, G.-l Assessment of potential biotoxicity induced by biochar-derived dissolved organic matters to biological fermentative H2 production. *Sci. Total. Environ.* **838**, 156072 (2022).
218. Ahmed, M. B., Zhou, J. L., Ngo, H. H., Guo, W. & Chen, M. Progress in the preparation and application of modified biochar for improved contaminant removal from water and wastewater. *Bioresour. Technol.* **214**, 836–851 (2016).
219. Enaime, G., Baçaoui, A., Yaacoubi, A. & Lübken, M. Biochar for wastewater treatment-conversion technologies and applications. *Appl. Sci.* **10**, 3492 (2020).
220. Zhao, M. et al. Mechanisms of Pb and/or Zn adsorption by different biochars: biochar characteristics, stability, and binding energies. *Sci. Total. Environ.* **717**, 136894 (2020).
221. Ihsanullah, I., Khan, M. T., Zubair, M., Bilal, M. & Sajid, M. Removal of pharmaceuticals from water using sewage sludge-derived biochar: a review. *Chemosphere* **289**, 133196 (2022).
222. Li, J., Chen, X., Yu, S. & Cui, M. Removal of pristine and aged microplastics from water by magnetic biochar: adsorption and magnetization. *Sci. Total. Environ.* **875**, 162647 (2023).
223. Silvani, L. et al. Characterizing biochar as alternative sorbent for oil spill remediation. *Sci. Rep.* **7**, 43912 (2017).
224. Pallewatta, S., Samarasekara, S. M., Rajapaksha, A. U. & Vithanage, M. Oil spill remediation by biochar derived from bio-energy industries with a pilot-scale approach during the X-Press Pearl maritime disaster. *Mar. Pollut. Bull.* **189**, 114813 (2023).

225. Sun, X. et al. Development of a new hydrophobic magnetic biochar for removing oil spills on the water surface. *Biochar* **4**, 60 (2022).
226. Navarathna, C. M. et al. Biochar adsorbents with enhanced hydrophobicity for oil spill removal. *ACS Appl. Mater. Interfaces* **12**, 9248–9260 (2020).
227. Sankaranarayanan, S., Lakshmi, D. S., Vivekanandhan, S. & Ngamcharussrivichai, C. Biocarbons as emerging and sustainable hydrophobic/oleophilic sorbent materials for oil/water separation. *Sustain. Mater. Technol.* **28**, e00268 (2021).
228. Gao, X. et al. Carbonaceous materials as adsorbents for CO_2 capture: synthesis and modification. *Carbon Capture Sci. Technol.* **3**, 100039 (2022).
229. Liu, S.-H. & Huang, Y.-Y. Valorization of coffee grounds to biochar-derived adsorbents for CO_2 adsorption. *J. Clean. Prod.* **175**, 354–360 (2018).
230. Cao, L. et al. Straw and wood based biochar for CO_2 capture: adsorption performance and governing mechanisms. *Sep. Purif. Technol.* **287**, 120592 (2022).
231. Presser, V., McDonough, J., Yeon, S.-H. & Gogotsi, Y. Effect of pore size on carbon dioxide sorption by carbide derived carbon. *Energy Environ. Sci.* **4**, 3059–3066 (2011).
232. Querejeta, N., Gil, M. V., Pevida, C. & Centeno, T. A. Standing out the key role of ultramicroporosity to tailor biomass-derived carbons for CO_2 capture. *J. CO2 Util.* **26**, 1–7 (2018).
233. Ma, X. et al. Heteroatom-doped porous carbons exhibit superior CO_2 capture and CO_2/N_2 selectivity: understanding the contribution of functional groups and pore structure. *Sep. Purif. Technol.* **259**, 118065 (2021).
234. Zhang, C., Sun, S., He, S. & Wu, C. Direct air capture of CO_2 by KOH-activated bamboo biochar. *J. Energy Inst.* **105**, 399–405 (2022).
235. Vargas, D. P., Giraldo, L. & Moreno-Piraján, J. CO_2 adsorption on granular and monolith carbonaceous materials. *J. Anal. Appl. Pyrolysis* **96**, 146–152 (2012).
236. Malode, S. J. et al. Biomass-derived carbon nanomaterials for sensor applications. *J. Pharm. Biomed. Anal.*, **222**, 115102 (2022).
237. Ouyang, C. & Wang, X. Recent progress in pyrolyzed carbon materials as electrocatalysts for the oxygen reduction reaction. *Inorg. Chem. Front.* **7**, 28–36 (2020).
238. Mian, M. M. & Liu, G. Recent progress in biochar-supported photocatalysts: synthesis, role of biochar, and applications. *RSC Adv.* **8**, 14237–14248 (2018).
239. Cai, X. et al. Chlorine-promoted nitrogen and sulfur co-doped biocarbon catalyst for electrochemical carbon dioxide reduction. *ChemElectroChem* **7**, 320–327 (2020).
240. Wang, D. et al. Co-embedded N-doped hierarchical porous biocarbons: facile synthesis and used as highly efficient catalysts for levulinic acid hydrogenation. *Fuel* **329**, 125364 (2022).
241. Zhang, X. et al. Enhancing the activity of Zn, Fe, and Ni-embedded microporous biocarbon: towards efficiently catalytic fast co-pyrolysis/gasification of lignocellulosic and plastic wastes. *Energy Convers. Manage.: X* **13**, 100176 (2022).
242. Wang, C. et al. Construction and synthesis of MoS_2/biocarbon composites for efficient visible light-driven catalytic degradation of humic acid. *Catalysts* **12**, 1423 (2022).
243. Xiong, X. et al. A review of biochar-based catalysts for chemical synthesis, biofuel production, and pollution control. *Bioresour. Technol.* **246**, 254–270 (2017).
244. Aman, A. M. N., Selvarajoo, A., Lau, T. L. & Chen, W.-H. Biochar as cement replacement to enhance concrete composite properties: a review. *Energies* **15**, 7662 (2022).
245. Liu, J. et al. Application potential analysis of biochar as a carbon capture material in cementitious composites: a review. *Constr. Build. Mater.* **350**, 128715 (2022).
246. Cuthbertson, D., Berardi, U., Briens, C. & Berruti, F. Biochar from residual biomass as a concrete filler for improved thermal and acoustic properties. *Biomass Bioenergy* **120**, 77–83 (2019).
247. Service, R. F. Electrified cement could turn houses and roads into nearly limitless batteries. *Science*, https://doi.org/10.1126/science.adk0583 (2023).
248. Sun, H., Hockaday, W. C., Masiello, C. A. & Zygourakis, K. Multiple controls on the chemical and physical structure of biochars. *Ind. Eng. Chem. Res.* **51**, 3587–3597 (2012).
249. Paula, A. J. et al. Machine learning and natural language processing enable a data-oriented experimental design approach for producing biochar and hydrochar from biomass. *Chem. Mater.* **34**, 979–990 (2022).
250. Kalak, T. Potential use of industrial biomass waste as a sustainable energy source in the future. *Energies* **16**, 1783 (2023).
251. Kamal Baharin, N. S. et al. Impact and effectiveness of bio-coke conversion from biomass waste as alternative source of coal coke in Southeast Asia. *J. Mater. Cycles Waste Manage.* **25**, 17–36 (2023).
252. Di Gruttola, F. & Borello, D. Analysis of the EU secondary biomass availability and conversion processes to produce advanced biofuels: use of existing databases for assessing a metric evaluation for the 2025 Perspective. *Sustainability* **13**, 7882 (2021).
253. Anastas, P. & Eghbali, N. Green chemistry: principles and practice. *Chem. Soc. Rev.* **39**, 301–312 (2010).
254. Don Taylor, G., English, J. R. & Graves, R. J. Designing new products: compatibility with existing production facilities and anticipated product mix. *Integr. Manuf. Syst.* **5**, 13–21 (1994).
255. Das, P., Banerjee, S. and Das, N. C. in *Polymer Nanocomposites Containing Graphene* (eds Rahaman, M., Lalatendu, N., Ibnelwaleed, A. H. & Das, N. C.) 683–711 (Elsevier, 2022).
256. Tripathi, N., Uribe, A. R., Weldekidan, H., Misra, M. & Mohanty, A. K. Upcycling of waste jute biomass to advanced biocarbon materials: the effect of pyrolysis temperature on their physicochemical and electrical properties. *Mater. Adv.* **3**, 9071–9082 (2022).
257. Li, Y. et al. Biochar as a renewable source for high-performance CO_2 sorbent. *Carbon* **107**, 344–351 (2016).
258. Hariram, M. et al. Novel puffball (*Lycoperdon* sp.) spores derived hierarchical nanostructured biocarbon: a preliminary investigation on thermochemical conversion and characterization for supercapacitor applications. *Mater. Lett.* **291**, 129432 (2021).
259. Sun, Q. et al. Bio-inspired heteroatom-doped hollow aurilave-like structured carbon for high-performance sodium-ion batteries and supercapacitors. *J. Power Sources* **461**, 228128 (2020).
260. Chen, W., Luo, M., Yang, K. & Zhou, X. Microwave-assisted KOH activation from lignin into hierarchically porous carbon with super high specific surface area by utilizing the dual roles of inorganic salts: microwave absorber and porogen. *Microporous Mesoporous Mater.* **300**, 110178 (2020).
261. García-Mateos, F. J. et al. Activation of electrospun lignin-based carbon fibers and their performance as self-standing supercapacitor electrodes. *Sep. Purif. Technol.* **241**, 116724 (2020).
262. Ma, X., Kolla, P., Zhao, Y., Smirnova, A. L. & Fong, H. Electrospun lignin-derived carbon nanofiber mats surface-decorated with MnO_2 nanowhiskers as binder-free supercapacitor electrodes with high performance. *J. Power Sources* **325**, 541–548 (2016).
263. Demir, M. et al. Lignin-derived heteroatom-doped porous carbons for supercapacitor and CO_2 capture applications. *Int. J. Energy Res.* **42**, 2686–2700 (2018).
264. Yin, W. M. et al. Fabrication of dually N/S-doped carbon from biomass lignin: porous architecture and high-rate performance as supercapacitor. *Int. J. Biol. Macromol.* **156**, 988–996 (2020).
265. Zhang, K. et al. High-performance supercapacitor energy storage using a carbon material derived from lignin by bacterial activation before carbonization. *J. Mater. Chem. A* **7**, 26838–26848 (2019).
266. Chen, F. et al. Self-assembly of NiO nanoparticles in lignin-derived mesoporous carbons for supercapacitor applications. *Green Chem.* **15**, 3057–3063 (2013).
267. Xu, J., Zhou, X., Chen, M., Shi, S. & Cao, Y. Preparing hierarchical porous carbon aerogels based on enzymatic hydrolysis lignin through ambient drying for supercapacitor electrodes. *Microporous Mesoporous Mater.* **265**, 258–265 (2018).
268. Wang, H. et al. Preparation of size-controlled all-lignin based carbon nanospheres and their electrochemical performance in supercapacitor. *Ind. Crop. Prod.* **179**, 114689 (2022).
269. Andooz, A., Eqbalpour, M., Kowsari, E., Ramakrishna, S. & Cheshmeh, Z. A. A comprehensive review on pyrolysis of E-waste and its sustainability. *J. Clean. Prod.* **333**, 130191 (2022).
270. Wunderlich, J., Armstrong, K., Buchner, G. A., Styring, P. & Schomäcker, R. Integration of techno-economic and life cycle assessment: defining and applying integration types for chemical technology development. *J. Clean. Prod.* **287**, 125021 (2021).
271. Li, W. et al. Regional techno-economic and life-cycle analysis of the pyrolysis-bioenergy-biochar platform for carbon-negative energy. *Biofuels Bioprod. Biorefin.* **13**, 1428–1438 (2019).
272. Matykiewicz, D. Biochar as an effective filler of carbon fiber reinforced bio-epoxy composites. *Processes* **8**, 724 (2020).
273. Ho, M.-P., Lau, K.-T., Wang, H. & Hui, D. Improvement on the properties of polylactic acid (PLA) using bamboo charcoal particles. *Compos. Part B* **81**, 14–25 (2015).
274. Zhang, Q. et al. Production of high-density polyethylene biocomposites from rice husk biochar: effects of varying pyrolysis temperature. *Sci. Total Environ.* **738**, 139910 (2020).
275. Das, O., Bhattacharyya, D., Hui, D. & Lau, K.-T. Mechanical and flammability characterisations of biochar/polypropylene biocomposites. *Compos. Part B* **106**, 120–128 (2016).
276. Romero Millan, L. M., Ghogia, A. C., White, C. E. & Nzihou, A. Iron nanoparticles to catalyze graphitization of cellulose for energy storage applications. *ACS Appl. Nano Mater.* **6**, 3549–3559 (2023).
277. Wang, L. et al. Mechanisms and reutilization of modified biochar used for removal of heavy metals from wastewater: a review. *Sci. Total Environ.* **668**, 1298–1309 (2019).
278. Tran, H. N. et al. Innovative spherical biochar for pharmaceutical removal from water: insight into adsorption mechanism. *J. Hazard. Mater.* **394**, 122255 (2020).
279. Qiu, B., Shao, Q., Shi, J., Yang, C. & Chu, H. Application of biochar for the adsorption of organic pollutants from wastewater: modification strategies, mechanisms and challenges. *Sep. Purif. Technol.* **300**, 121925 (2022).
280. Serafin, J., Narkiewicz, U., Morawski, A. W., Wróbel, R. J. & Michalkiewicz, B. Highly microporous activated carbons from biomass for CO_2 capture and effective micropores at different conditions. *J. CO2 Util.* **18**, 73–79 (2017).
281. Petrovic, B., Gorbounov, M. & Soltani, S. M. Impact of surface functional groups and their introduction methods on the mechanisms of CO_2 adsorption on porous carbonaceous adsorbents. *Carbon Capture Sci. Technol.* **3**, 100045 (2022).
282. Das, O. & Bhattacharyya, D. in *Interface/Interphase in Polymer Nanocomposites* (eds Netravali, A. N. & Mittal, K. L.) 333–374 (Scrivener Publishing, 2016).
283. Oliver, W. C. & Pharr, G. M. An improved technique for determining hardness and elastic modulus using load and displacement sensing indentation experiments. *J. Mater. Res.* **7**, 1564–1583 (1992).
284. Bhushan, B. & Koinkar, V. N. Nanoindentation hardness measurements using atomic force microscopy. *Appl. Phys. Lett.* **64**, 1653–1655 (1994).

Acknowledgements

The authors thank the Ontario Research Fund, Research Excellence Program; Round 9 (ORF-RE09) Ontario Ministry of Colleges and Universities; the Ontario Ministry of Agriculture, Food and Rural Affairs (OMAFRA)–University of Guelph–Ontario Agri-Food Innovation Alliance; the Natural Sciences and Engineering Research Council of Canada (NSERC);

and the Agriculture and Agri-Food Canada (AAFC) through Bioindustrial Innovation Canada (BIC) Bioproducts AgSci Cluster Program for financial support.

Author contributions

Conceptualization of the article (A.K.M., M.M., O.D. and S.V.); Introduction (A.K.M., S.V. and O.D.); Experimentation (A.N., S.V., O.D., N.B.K., L.M.R.M. and M.M); Results (O.D., S.V., A.K.M., L.M.R.M., N.B.K., A.N. and M.M.); Applications (S.V., O.D., A.K.M., N.B.K., A.N., L.M.R.M. and M.M.); Reproducibility and data deposition (L.M.R.M., N.B.K., O.D. and S.V.); Limitations and optimizations (O.D., S.V., N.B.K., A.N. and M.M.); Outlook (S.V., O.D., A.N., A.K.M. and M.M); overview of the Primer (all authors).

Competing interests

The authors declare no competing interests.

Additional information

Supplementary information The online version contains supplementary material available at https://doi.org/10.1038/s43586-024-00297-4.

[1]Bioproducts Discovery and Development Centre, Department of Plant Agriculture, University of Guelph, Guelph, Ontario, Canada. [2]School of Engineering, University of Guelph, Guelph, Ontario, Canada. [3]Sustainable Materials and Nanotechnology Lab (SMNL), Department of Physics, V.H.N.S.N. College (Autonomous), Virudhunagar, Tamil Nadu, India. [4]Department of Civil, Environmental and Natural Resources Engineering, Luleå University of Technology, Luleå, Sweden. [5]Universidad Nacional de Colombia – Sede Bogotá, Facultad de Ingeniería, Ciudad Universitaria, Bogotá, Colombia. [6]Department of Chemical and Biochemical Engineering, The University of Western Ontario, London, Ontario, Canada. [7]Institute for Chemicals and Fuels from Alternative Resources (ICFAR), The University of Western Ontario, London, Ontario, Canada. [8]IMT Mines Albi, RAPSODEE CNRS UMR 5302, Université de Toulouse, Campus Jarlard, Toulouse, France. [9]Andlinger Center for Energy and the Environment, Princeton University, Princeton, NJ, USA.